Final Report to US Department of Energy

Project Nos. DE-FG02-96ER12184 and DE-FG26-97FT97268

Supported Molten Metal Catalysis. A New Class of Catalysts

Ravindra Datta,[#] Ajeet Singh, Manuela Serban,[*] and Istvan Halasz[✡]

Fuel Cell Center, Department of Chemical Engineering, Worcester Polytechnic Institute, Worcester, MA 01609

[*] *UOP, 25 E. Algonquin Rd, 2B-119 Research Bldg, Des Plaines, IL 60017*

[✡] *The PQ Corp., R & D, 280 Cedar Grove Road, Conshohocken, PA 19428*

[#] Email: rdatta@wpi.edu; Tel: 1-508-831-6036

Supported Molten Metal Catalysis. A New Class of Catalysts

Ravindra Datta,[#] Ajeet Singh, Manuela Serban,[*] and Istvan Halasz[✡]

Fuel Cell Center, Department of Chemical Engineering, Worcester Polytechnic Institute, Worcester, MA 01609

[*]*UOP, 25 E. Algonquin Rd, 2B-119 Research Bldg, Des Plaines, IL 60017*

[✡]*The PQ Corp., R & D, 280 Cedar Grove Road, Conshohocken, PA 19428*

Abstract

We describe a new class of heterogeneous catalysts called supported molten metal catalysis (SMMC), in which molten metal catalysts are dispersed as nanodroplets on the surface of porous supports, allowing much larger active surface area than is possible in conventional contacting techniques for catalytic metals that are molten under reaction conditions, thus greatly enhancing their activity and potential utility. Specific examples of different types of reactions are provided to demonstrate the broad applicability of the technique in designing active, selective, and stable new catalysts. It is shown that dispersing the molten metal on a support in the suggested manner can enhance the rate of a reaction by three to four orders of magnitude as a result of the concomitant increase in the active surface area. New reaction examples include γ-Al_2O_3 supported molten Te (melting point 450 ºC) and Ga (MP 30 ºC) catalysts for bifunctional methylcyclohexane dehydrogenation. These catalysts provide activity similar to conventional Pt-based catalysts for this with better resistance to coking. In addition, results are described for a controlled pore glass supported molten In (MP 157 ºC) catalyst for the selective catalytic reduction of NO with ethanol in the presence of water, demonstrating activities superior to conventional catalysts for this reaction. A discussion is also provided on the characterization of the active surface area and dispersion of these novel supported catalysts. It is clear based on the results described that the development of new active and selective supported molten metal catalysts for practical applications is entirely plausible.

Keywords: Heterogeneous catalysis, supported catalysts, supported liquid catalysts, supported molten metal catalysts, molten metals, molten alloys, dehydrogenation, SCR

[#] Email: rdatta@wpi.edu; Tel: 1-508-831-6036

1 Introduction

Heterogeneous metal catalysis is the backbone of the chemical industry [1]. It functions via the ability of the catalyst surface to form bonds of intermediate strength with the reactants by sharing of electrons between the metal and the reacting species, thereby allowing internal rearrangement of the reactant bonds to form products that subsequently desorb from the surface. Transition metals appear to make the most active catalysts for many reactions of industrial interest. Since many of these are expensive materials, engineering considerations require a large surface area in a small volume. This is accomplished via the dispersion of nanometer-sized particles [2] of the catalytic material on nanoporous inorganic supports, thus providing a very large active area for a small amount of the catalyst. This not only allows economic use of the catalytic materials and practical conversions in small catalytic fixed-bed reactors, but provides facile separation of the catalyst from the reacting species. In fact, the development of supported heterogeneous catalysis ranks as one of the key technological accomplishments of the twentieth century, making it practical to use expensive catalytic materials in a host of industrial chemical and petrochemical processes.

However, heterogeneous catalysts often provide limited selectivity to the desired product due to a variety of crystal faces on the nanocrystallite surface, that bind with different strength and hence possess different activity and selectivity. Further, many heterogeneous catalysts in use have limited resistance to poisoning and sintering. Thus, a key goal of research in the 21st century is to design catalysts with better stability and selectivity [3], due to increasing attention to environmental and resource conservation issues.

Homogeneous catalysts (liquid phase) are promising toward the accomplishments of these goals, providing high catalyst activity as well as product selectivity under mild operating conditions, because it is possible to precisely tailor the nature of the catalytic site [4]. However, the application of homogeneously catalyzed reactions in industry has so far been limited owing to some practical problems associated with their usage. Thus, separation of the homogeneous catalysts from the reaction mixture is often difficult. Lack of effective catalyst utilization in conventional gas-sparged reactor, corrosion problems, and catalyst contamination in the product are among the other disadvantages of homogeneous catalysis.

As a result, there have been numerous attempts to “heterogenize” the liquid phase catalysts [5], so that the resulting catalysts would have the advantages of both homogeneous and heterogeneous catalysts, namely, high activity and selectivity, ease of separation, and non-corrosive environment. The various techniques investigated include ligand attachment to the support either via a covalent [6] or ionic bond [7], supported liquid-phase catalysis (SLPC) [8-12], supported aqueous-phase catalysis (SAPC) [13, 14], supported molten-salt catalysis (SMSC) [15, 16], and supported ionic liquid catalysis (SILC) [17], wherein nano-films of high-boiling organic or aqueous solvent, or molten salt or room temperature ionic liquid, are coated on the walls of porous support. Most of these techniques, based on the original idea of Rony [8], show growing promise, although they each have their limitations as well, especially in terms of stability when the supported liquid has significant volatility or solubility in the reacting phase.

Here, we report on a new technique called supported molten metal catalysis (SMMC) [18 - 20], wherein nano-droplets or nano-films of molten catalytic metals or alloys are dispersed on high surface area refractory supports to provide a new class of heterogeneous catalysts. Industrial catalytic reactions generally proceed at elevated temperatures, typically in the range of 300 - 600 ºC, and sometimes up to 1,000 ºC, as for example in solid oxide fuel cells and reforming reactions. At these temperatures, many catalytic metals and alloys of potential interest are molten [21], thus precluding their use in industrial practice. Thus, although liquid metal and alloy catalysis has been investigated for the past century for a number of reactions [21], so far there has been little use for these materials because of significant issues associated their use of limited active area and severe corrosion. All of these problems can be effectively overcome via the technique of supported molten metal catalysis (SMMC) described here, that allows the use of a broad range of novel catalytic materials not employed so far.

2 Molten Metal Catalysis

The catalytic properties of liquid metals and alloys have attracted attention of a handful of investigators since the turn of the last century, when it was discovered that metallic zinc catalyzed the decomposition of alcohols above its melting point [22]. Later on, no discontinuity in its activity was found above and below the melting point of zinc for the thermal decomposition of methyl alcohol [23]. Other molten metal surface catalyzed reactions investigated early on include reduction of nitrobenzene to aniline over molten cadmium, lead,

thallium, and bismuth [24], catalytic oxidation of ammonia over fused metallic tin and silver [25], and hydrogenation of polynuclear aromatic compounds over molten alkali metals and alloys [26].

More recent work on molten metal catalysis is summarized in the monograph by Ogino [21], whose group has extensively investigated catalytic activities of various metals and semi-metals such as Na, K, Zn, Cd, Hg, Al, Ga, In, Tl, Sn, Pb, Sb, Bi, Te and Se, with melting points in the range of −39 ºC to 660 ºC, as well as some binary molten alloys. They found many molten metal catalysts to be highly selective as well as stable. The various types of reactions systematically investigated by Ogino and co-workers [21] include dehydrogenation of alcohols, amines, and hydrocarbons, hydrogenation of hydrocarbons, hydrogen transfer reactions, and coal liquefaction.

A key question, of course, is whether molten metal catalysts are fundamentally different from conventional heterogeneous metal catalysts. This is addressed below to the extent possible with the current state of knowledge keeping in mind that, in fact, there is no universally accepted theory of catalysis, the catalyst development so far having been largely empirical. Nonetheless, there are semi-empirical correlations and heuristics that provide useful guidance in catalyst design. These include the so-called volcano plots, Sabatier principle, Evans-Polanyi relation, binding energy trends across the periodic table, *d*-band energy, Fermi level, and work function, etc [1, 27]. Furthermore, lately, there has been a substantial increase in the application of quantum chemical theory to develop an improved understanding of heterogeneous catalysis. The limited results available so far also seem to support the above heuristics [28, 29], e.g., volcano plots may be explained on the basis of the adsorbate-metal bond strength, which in turn may be related to the average energy of *d* states relative to Fermi level, $\varepsilon_d - \varepsilon_F$ [28].

The best guide, therefore, appears to be the position of the metal in the periodic table and its electronic properties. Relation to electronic properties is also found for molten metals. Thus, a close parallel between the work function and 2-butanol dehydrogenation activity was found, as the work function changed for a series of In-Sn liquid alloys of varying composition [21]. Further, a quantum chemical study of alcohol dehydrogenation over molten metal also suggests that the electron localization from the metal to the adsorbate is facilitated as the Fermi level of the metal increases [21]. Thus, electron donating properties of liquid metals appear closely related to their catalytic activity. In other words, there appears to be no fundamental difference

between liquid metal and solid metal catalysis, in that the catalysis proceeds via surface-adsorbate interaction, which in turn is related to its electronic properties. The latter, of course, can be controlled via alloying.

A related question is whether the electronic and other relevant properties of a metal change significantly upon melting. Results based on photoelectron spectroscopy suggest that the band structure of electron energies of a metal does not collapse on melting, even though fine features of energy distribution curve do change, suggesting that the short-range order of atoms persists on melting [21]. The work function of the metal also does not vary significantly upon phase change [21]. From this discussion, nothing unusual is expected in molten metal surface catalysis, apart from the properties indicated by the position of the element in the periodic table.

The molten metal catalyzed reactions have so far been studied in reaction vessels containing a pool of molten metal with reacting gases being passed over it or bubbled through it (Figure 1) [21]. When used in this form, there are severe limitations on the rate of reaction due to the very small active area obtained. This greatly reduces the effectiveness of catalyst utilization, requiring large reactors for a given conversion. In fact, only fast reactions can be investigated in this manner because of the very limited active area available (Figure 1). Furthermore, handling and corrosion with molten metals present very serious challenges. These stumbling blocks, however, can be effectively overcome by the SMMC technique.

3 Supported Molten Metal Catalysis

In the supported molten metal catalysis (SMMC) technique (Figure 2) [18 – 20], the molten metal or alloy catalyst is dispersed on the large internal pore surface area of a porous refractory support either as (a) nano-droplets or as (b) fragmented or (c) continuous nano-films depending upon the wetting characteristics of the melt and the amount of metal loading. The molten metal droplets or films are held in place by van der Waals and surface tension forces. The reactants diffuse through the residual pore space and react on the *surface* of the liquid metal catalyst. This is distinct from supported homogeneous catalysts (i.e., SLPC, SMSC, SAPC, SILC, etc.), where reactants dissolve within the supported film and react *homogeneously* within the liquid phase. In other words, SMMC is a class of heterogeneous, rather than homogeneous, catalysts, despite the physical similarity of the technique with SLPC, SMSC, etc. As a result, the optimum amount of liquid metal loading corresponds to that providing the largest specific surface area (m^2/g), rather

than the maximum volume that can be supported without being substantially restricted by increased diffusion limitations due to constriction of remaining pore space [10, 12, 15].

Various techniques such as the conventional precursor solution impregnation followed by reduction, melt imbibition, vapor deposition, etc., could be used to coat the molten metal or alloy on the internal surface of porous support. The materials that are suited for the SMMC technique include metals, semimetals, and their alloys that are molten under typical reaction conditions. Further, crystallites of metal and/or metals salts catalysts may be readily dispersed in the molten metal catalyst for rate or selectivity enhancement through synergism or for bifunctional catalysis. The crystallites of metals suitable for dispersion may be conventional catalysts such as platinum, palladium, rhodium, nickel, and silver. In addition, active oxides, e.g., CeO_2, or Cr_2O_3, may be dispersed.

The SMMC technique provides the following advantages:

1. Large catalytic activity per unit mass of the molten metal catalyst due to the high dispersion, as compared with the usage of molten metals in bulk form.
2. High rates of reaction per unit volume of reactor, once again due to the high efficiency of catalyst utilization.
3. Almost a complete absence of corrosion problems since the molten metal is confined within the pores of the refractory support and does not come in direct contact with the reactor walls.
4. The technique offers atomically uniform surface for catalysis unlike conventional heterogeneous catalysts that contain different crystal faces.
5. No sophisticated techniques are necessary for preparing the catalysts.
6. The deactivation due to sintering, common in solid metal catalysis, is avoided.
7. Since the catalyst surface sites are mobile, they are subject to renewal and hence conceivably they are less susceptible to fouling, for instance due to carbonaceous deposition.
8. The mobile nature of the surface likely also affects reaction rates and selectivities, especially for reactions on sites involving atomic ensembles. Of course, more recent surface science and *ab initio* work indicates that the catalyst sites on conventional heterogeneous catalysts are also not frozen but rather undergo dynamic restructuring upon adsorption and surface reaction [30].

9. The technique provides an opportunity to investigate reactions not so far studied on molten metal catalysts due to much higher surface area and possibility of bifunctional catalysis with support afforded by the SMMC technique.

3.1 Molten Metals

A large variety of molten metals, alloys, semimetals, and intermetallic compounds is available with melting points ranging from below room temperature up to 1000 ºC. The metals of interest for use in SMMC range from groups 1, 12, 13, 14, 15, 16 of the periodic table [21]. Some of the possible molten metals and alloys that may be used in SMMC system are given in Tables1 and 2, respectively. The melting and the boiling points of some of the metals of interest are shown in Figure 3 (a) versus their electronic configuration, the latter determining their catalytic properties. An interesting linear relationship between melting point and enthalpy of formation of gas phase metal atoms across the periodic table is shown in Figure 3 (b). The melting point first increases and then decreases from left to right across the periodic table [18]. The enthalpy of formation of metal in the gas phase also first increases and then decreases as one moves from left to right across the periodic table. As a result, there is a linear correlation between the two. These trends, while not fully understood yet, may be significant as further progress is made in the design of SMMC.

Metals with a melting point below 500 ºC, and those with the largest liquidous range, *i.e.*, those that have the largest difference between the boiling and melting points, and hence probably the lowest vapor pressures (Figure 4) [31] under reaction conditions, are the most desirable for SMMC, so as to avoid loss of catalyst from support due to volatility. For instance, Indium, which has a melting point of 156.4 $^{\circ}$C and vapor pressure of 10^{-8} torr at 770 $^{\circ}$K, is a suitable metal for SMMC system. In addition, of course, alloying can dramatically change the physical (MP, BP, vapor pressure, etc.) as well as electronic or catalytic properties of the catalyst. Thus, melting points of some binary and ternary liquid alloys with relatively low melting points are provided for illustrative purposes in Table 2 [32].

3.2 Porous Supports

A variety of commercially available porous supports (Table 3) may, of course, be used for preparation of SMMC [33], depending upon the metal, and the type of reaction for which the

catalyst is intended to be used. The choice of the support is based on the following criteria: surface area, porosity and pore size distribution, inertness, mechanical strength, *e.g.*, hardness, attrition resistance, stability under reaction conditions, and dual functionality, if desirable. The wetting of the support by the molten metal is another important criterion for SMMC preparation. For coating a thin film of liquid metal on a porous support surface, the contact angle between liquid metal and support should be less than 90 º [10] and liquid metal should have high work of adhesion. Although liquid metals typically do not wet (contact angle > 90 º) silica or alumina substrates [20, 34], one can still expect good dispersion when the adhesion is strong enough to provide small liquid metal droplets on the surface, much like the supported micro-crystallites of traditional solid metal catalysts.

3.3 SMMC Preparation

A number of different methods such as vapor deposition, solution impregnation, or melt imbibition, could be used for SMMC preparation, the suitability of the different methods depending upon the physical and chemical properties of the molten metal and the support [20]. The vapor deposition method consists of heating the catalyst support and metal catalyst in a closed inert atmosphere at a temperature high enough to produce sufficient vapor pressure of the metal catalyst. There are, of course, alternate methods of producing the metal vapor, e.g., sputtering or laser ablation. The metal vapors then diffuse into the pores of the support and, on cooling, get deposited on the pore walls of the support.

The solution impregnation method is commonly used in the preparation of conventional heterogeneous catalysts and involves soaking the porous carrier in a solution of the appropriate metal salt, followed by drying and then reducing the deposited salt to the corresponding metal [33]. As an example, a Te-Al_2O_3 catalyst was prepared [18] by dissolving an appropriate amount of telluric acid in warm water at about 50-60 $^{\circ}$C, and immersing the porous γ-Al_2O_3 support (United Catalysts, Inc., T-374) in the solution overnight. Pellets thus loaded with telluric acid solution were placed in a vacuum oven at ambient temperature for about 12 hours to remove water and deposit telluric acid inside the pores of the support. Telluric acid was next reduced to active Te metal inside the pores of the support by contacting with 10-12% solution of hydrazine for about 10 hours.

The melt imbibition method is unique to SMMC. In this method, appropriate amounts of catalyst support and metal catalyst in powder form are mixed and heated together above the melting point of the metal, either in an inert atmosphere, or in air. Since not all supports would take up the molten metal via this technique, a transparent furnace was designed (Figure 5) to help in visualizing the interaction between various metals and supports in an air-free environment, at elevated temperatures [20]. The molten metal comes directly into contact with the porous support, which allows molten metal uptake by capillary action and dispersion by surface tension. The metal loading is confirmed by weight change.

4 SMMC Physical Characterization

The physical characteristics in terms of nano-particle size, dispersion, active area, BET area, and pore size distribution, as they change with metal loading, were determined as follows. For this purpose, controlled pore glass (CPG) (Sigma Chemical Co.) was used because of its high surface area (~ 170 m^2/g), and its well-characterized and largely uniform pores (64 Å radius). Thus, a series of supported molten In and Ga catalysts on CPG were prepared by the melt imbibition method, and denoted as In-CPG-SMMC and Ga-CPG-SMMC, respectively. For varying metal loading, fractions of calculated monomolecular coverage were used. For a theoretical monomolecular coverage for In and Ga on the 170 m^2/g CPG, a loading is needed of 28 and 24 w%, respectively. Therefore, the metal concentrations in the In and Ga based SMMCs were varied by using fractions these upper concentrations. Thus, the In-CPG-SMMC samples studied contain 28, 14, 7, 1.8, and 0.95 w% In.

4.1 BET Surface Area, Pore Volume, and Pore Size Distribution

BET surface area, pore volume and pore size distribution measurements were done in an adsorption/catalytic reactor system [20], as shown in Figure 6, involving a quartz reactor of approximately 5 cm^3 volume. The system is designed to operate over a wide pressure range, *i.e.*, from 1 x 10^{-8} up to 30 atm (1 x 10^{-10} to 3 x 10^3 kPa) to permit *in situ* catalyst physical and chemical characterization, including differential and integral kinetics. All parts of the system are corrosion resistant. The system is equipped with an Alcatel type Drytel Micro (5011) ceramic roughing pump plus molecular drag high vacuum pump. The high vacuum environment assures clean catalyst and support surfaces for *in situ* catalyst characterization before and after activity and kinetic measurements. The system is highly leak tight (pressure change < 10^{-5} torr/min when

evacuated to 10^{-6} torr). The manifold is made of stainless steel Swagelok bellow seal valves for alternate use of vacuum, pressure, and a variety of gas mixtures. The gaseous reactants are fed to the reactor through mass flow controllers (MKS type 1179A), while the liquid reactants are fed either with a Gilson model 302 high pressure liquid pump (0.01 – 5 ml/min. head) or with a stainless steel saturator connected to a Fisher Scientific liquid bath. An Omega model PX-931 solid-state pressure transducer (accuracy ± 0.25 %) is used for measuring pressures above 1 atm, while two heated (for minimum adsorption) Baratron type 128A solid state pressure transducers are used for reading sub-atmospheric pressures (accuracy ± 0.15 %). The mass flow controllers and the pressure transducers are connected to appropriate power-supply/readout units (MKS model 247C, MKS model PDR-C/2C). The temperature is controlled with an Omega CN76000 type temperature controller connected to a cylindrical furnace.

Prior to all measurements, the catalysts were pretreated in an identical manner. Thus, approximately 0.1 cm^3 of supported catalyst was loaded into the quartz reactor, evacuated at 10^{-6} torr at around 200 ºC to eliminate water vapors, then heated at 550 ºC, under helium flow. The samples were then reduced in a flow of 100 cm^3/min H_2 at 0.1 MPa for 60 minutes. Finally, the samples were again evacuated at 10^{-6} torr, and cooled down to liquid nitrogen temperature (77 K).

A typical set of nitrogen adsorption/desorption isotherms at – 196 ºC is shown in Figure 7(a), and the corresponding BET plot [35] for the 28 w% In-CPG-SMMC sample is shown in Figure 7(b). The plots demonstrate the high accuracy possible with the apparatus, with less than 2 % deviation being observed in repeated measurements.

For calculating the pore volume and pore size distribution of the In-CPG-SMMC samples, Dollimore and Heal's method was used [35], with the data points for pore size distribution analysis taken from the desorption branch of the isotherm. Figure 8 illustrates that the pore size distributions of the In-CPG-SMMC samples thus obtained are very similar to that of the original support even at high metal loadings. Thus, the majority of pores remain open, permitting easy access for reactants. A slight increase in the average pore size, with increasing In-content indicates that some fine pores might be getting filled up or clogged by the larger metal micro-droplets. Table 4 shows that increasing In loading substantially decreases the specific surface area and pore volume of the catalysts. Since most pores remain open, the decreasing pore volume implies that the diameter of many In droplets is smaller than the average pore diameter

even in the heavily loaded 28 w% In-CPG-SMMC sample. Thus, most droplets mainly reside on the walls of the pores. However, Table 4 also indicates that the drop in the pore volume of the support is somewhat bigger than the total volume of the loaded indium. Consequently, some large particles clog the entrance to some of the micropores and/or mesopores.

4.2 Chemisorption and Molten Metal Dispersion

Selective gas chemisorption allows determination of the number of surface sites and hence calculation of turnover frequencies in catalytic reactions [36]. Although hydrogen is a common adsorbate for chemisorption studies of precious metal catalysts, the adsorbing gas for our chemisorption studies with SMMC was chosen to be oxygen, since it is the easiest molecule to activate and adsorb on metal surfaces, and is suitable for mildly reactive catalysts as well. The chemisorption measurements were made in the above described apparatus on three catalysts prepared by the melt imbibition method with different metal loadings, namely, a 14 w%, a 1.75 w%, and a 0.95 w% In-CPG-SMMC. Before measurement of oxygen isotherms, the catalysts were subjected to the standard pretreatment described above. The stainless steel manifold was also heated during the evacuation, to avoid any possible adsorption on it. The amount of oxygen adsorbed on the support itself was found in all cases to be small (< 0.1 μmol $O_2/g_{support}$). To account for this, for each sample, the oxygen adsorption was measured twice. Thus, after the first adsorption (chemisorption + physisorption), the samples were evacuated for 30 minutes at the temperature of the measurement and a second adsorption was done. During the evacuation, the oxygen molecules weakly held by van der Waals forces were released, such that in the second adsorption the amount of oxygen physisorbed could be measured directly. Taking the difference between these two adsorption measurements, the chemisorption isotherm could be obtained. Adsorption isotherms were thus determined for each catalyst at several temperatures.

Figure 9(a) shows the chemisorption isotherms for a 1.75 w%, In-CPG-SMMC at different temperatures, in the oxygen pressure (P_e) range 0 - 10 Torr. These data conform well to Freundlich isotherm, in the pressure range covered, described by [37]

$$q_a = CP_e^{\frac{1}{n}} \qquad (1)$$

where q_a is the amount adsorbed. The coefficients C and n are functions of temperature [37]. The coefficient n is as a measure of the affinity of the surface toward O_2 adsorption. Assuming that the Freundlich isotherm is followed in the entire range, it may be rearranged in the manner

$$\ln q_a = \ln C + \frac{1}{n}\ln P_e \qquad (2)$$

with $\ln C = \ln q_\infty - \frac{1}{n}\ln P_\infty$, *i.e.*, the coefficient C can be expressed in terms of q_∞, the amount adsorbed at monolayer coverage (θ = 1) corresponding to a pressure P_∞. Equation (2), thus, requires that a family of isotherms at different temperatures cross at a common point at a pressure P_∞, where the monolayer coverage is reached [38].

Figure 9(b) shows such a linearized Freundlich plot as per Eq. (2) for the 1.75 w% In-CPG-SMMC, at five different temperatures from which C and n may be determined at each temperature. As can be observed, the Freundlich equation is obeyed well and, furthermore, the family of isotherms appears to be crossing at a common point. From the plot shown in Figure 9-b, thus, the monolayer coverage for 1.75 w% In-CPG-SMMC was calculated to be 24 μmol O_2/g_{cat} and P_∞ = 1375 Torr. For 0.95 w% and for 14 w% In-CPG-SMMC, the monolayer coverages were similarly calculated to be 16.1 μmol O_2/g_{cat} (P_∞ = 1012 Torr) and 66.5 μmol O_2/g_{cat} (P_∞ = 2193 Torr), respectively.

Assuming that one In surface atom adsorbs one oxygen atom, *i.e.*, O_2 adsorbs dissociatively, the dispersion D of In on the porous glass support can be calculated as defined

$$D = \frac{n_S^M}{n_T^M} \qquad (3)$$

where n_S^M and n_T^M are the numbers of surface metal atoms and the total metal atoms [36]. The dispersions thus obtained for the three catalysts are: 39 % for the 0.95 w% In-CPG-SMMC, 32 % for the 1.75 w% In-CPG-SMMC and 11 % for the 14 w% In-CPG-SMMC, respectively. These are of the same order as in conventional supported solid metal catalysts. This, of course, is based on the assumption that the assumed stoichiometry is valid and that adsorption is limited to the surface layer, which may not be true, especially above the melting point of In. Interstitial oxygen is not uncommon on conventional catalysts either [27]. It may be noted however, that although the temperature range of chemisorption experiments spanned the In melting point (156.6 ºC), no discontinuity in the adsorption isotherm was observed. Further, the dispersion remained unchanged above and below the melting point.

The average nano-droplet diameter, d_M, assuming spherical shape, may also be calculated by means of [36]:

$$d_{\mathrm{M}} = 6\frac{\mathrm{V}_{\mathrm{sp}}}{S_{\mathrm{M}}} \qquad (4)$$

where S_M is the specific surface area of the metal, obtained from chemisorption data and assuming an average surface number density, *i.e.*, 10^{15} atoms/cm^2, and V_{sp} is the specific volume of the metal. The, thus, calculated nano-droplet average diameters are 4.9 nm, 5.8 nm, and 17 nm for the 0.95 w% In-CPG-SMMC, 1.75 w% In-CPG-SMMC, and 14 w% In-CPG-SMMC respectively. The sizes again compare favorably with the typical nano-crystallite size in conventional heterogeneous catalysts, implying that it is indeed possible to effectively disperse molten metals in the manner of solid metal catalysts.

4.3 Electron Microscopy and X-Ray Microanalysis

Samples of In-CPG-SMMC of different loadings prepared by the melt imbibition method were characterized by scanning electron microscopy (SEM) and X-ray microanalysis techniques. Since these catalysts are molten at reaction temperatures, we tried to simulate the catalyst under such conditions by immediately immersing the samples into liquid nitrogen after heating them above the melting point of In (156.6 ^{o}C). The SEM pictures were taken using a Hitachi S4000 SEM at an accelerating voltage of 5 kV. The samples were carbon coated to increase conductivity and to avoid cluttering of elemental lines to X-ray microanalysis spectra. The scanning electron micrograph of the largest loading (28 w%) In-CPG-SMMC is presented in Figure 10 (a). As can be seen, indium is dispersed on the porous CPG surface as microdroplets of diameters <1.4 μm at this high loading. Indium apparently distributes and adheres well on the CPG support surface even though the contact angle between the metal and support is > 90^{o}. The results of the X-ray microanalysis show that indium is distributed uniformly.

To confirm the presence of smaller droplets a Ga/γ-Al_2O_3 catalyst (10% loading), prepared by gallium nitrate solution impregnation method [18], was investigated by transmission electron microscopy (TEM) and energy dispersive X-ray (EDX) spectroscopy. Figure 10 (b) shows nano-droplets of Ga in the range of 4-20 nm size. The EDX spectrum for these droplets confirmed the metallic Ga phase. The TEM analysis of a number of samples showed the presence of well-dispersed small as well as larger gallium droplets.

5 Reaction Systems Investigated

Two type of examples of reactions investigated are provided below: 1) those reactions which have previously been investigated in molten metal pool reactors (Figure1), in order to show the dramatic enhancement in rates of reactions possible by virtue of the increased catalyst dispersion in SMMC (Figure 2) and the resulting huge increase in the active area; and 2) new reactions which could not have been observed in conventional pool reactors due to the very low active area available or are bifunctional in nature, involving also the activity of the support.

Before a discussion of the results, some of the terms are defined. Both integral (large conversion) and differential (low conversion) catalytic packed-bed reactor experiments were conducted, the former to check and compare reactivity of a catalyst, while the latter is for determining catalytic kinetics. The rate of a reaction (moles of R converted/g catalyst.s) was determined from differential conversion X of the key reactant R obtained from gas chromatography over a catalyst of mass W at a molar feed flow rate F_R

$$-r_R = \frac{F_R}{W} X \tag{5}$$

A useful representation of kinetics is in terms of an atomic rate, r_A (molecules of R converted/atom catalyst.s) calculated from

$$r_A = \frac{r_R (AW_M)}{\omega_M} \tag{6}$$

where AW_M is the atomic weight of the metal catalyst and ω_M is the w% catalyst loading. Finally the turnover number, N_T, or turnover frequency (TOF) was determined from

$$N_T = \frac{r_A}{D} \tag{7}$$

where D is the catalyst dispersion.

The selectivity S was calculated as the ratio of the rate of the conversion of reactant to the desired product to the total rate of the reactant conversion. Another term used is the weight hourly space velocity (WHSV) defined as the ratio of the mass flow rate of the reactant to the mass of the catalyst in the reactor.

5.1 Tetralin Dehydrogenation

This example demonstrates the dramatic enhancement in reaction rate possible as a result of increased dispersion and surface area in SMMC. Dehydrogenation of Tetralin, along with other

polynuclear hydrocarbons, was studied by Ogino and co-workers on liquid semimetal Te catalyst both in a bubbling type reactor, i.e., Figure 1(a) [39], as well as in a duct reactor, Figure 1(b) [40]. The reaction is illustrated below:

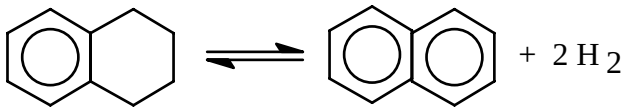

Tetralin Naphthalene

Since the surface area of the liquid Te catalyst in the duct reactor is known precisely, it was possible to calculate the turnover number or frequency, N_T, defined as the molecules of reactant converted per surface site (metal atom) per second, from the experiment data of Takahashi and Ogino [40]. The results as shown in Figure 11 in the temperature range of 508 ºC to 570 ºC.

It is of interest to compare this turnover number with that for the conventional transition metal catalysts, e.g., Pt/γ-Al_2O_3. Although comparable numbers for this particular reaction are not available in the literature, Somorjai [41] has summarized turnover numbers for the common hydrocarbon reactions on platinum catalysts. He gives an upper limit of $N_T < 100$ for the dehydrogenation reactions, which is of the order in Figure 11. Thus, Te appears to be a highly active for the dehydrogenation of tetralin.

The dehydrogenation of tetralin on a Te-supported molten metal catalyst was studied in the temperature range of 530 ºC to 595 ºC by utilizing a 3% Te/γ-Al_2O_3 catalyst prepared by the melt imbibition method. The results, in terms of an atomic rate, r_A, defined as molecules of reactant converted per bulk metal atom per second, are shown in Figure 12 and are also compared with the data of Takahashi and Ogino [39]. Figure 12 shows that the atomic rate in Te-supported molten metal catalyst is 3 to 4 orders of magnitude higher than that in unsupported Te, clearly demonstrating the dramatic enhancement in rate as a result of the increased surface area of supported catalyst in supported molten metal catalyst, thus establishing the basic efficacy and soundness of rationale of the SMMC technique.

The atomic rate data and turnover number can provide an indirect estimation of the dispersion D via Eq. (7). Thus, assuming that the turnover number, $N_T = 118$ at 570 ºC (Figure 11) remains unchanged over unsupported and supported molten metal, and for an atomic rate r_A = 15 molecules/metal atom.s at this temperature (Figure 12), the resulting dispersion, $D = 12.7\%$, indicating an average nano-droplet size of 12.5 nm. These numbers are consistent with the

dispersion determined via chemisorption as described above. Furthermore, the dispersion and particle size are of the same order as in conventional heterogeneous catalysis.

5.2 Ethanol Dehydrogenation

Ethanol dehydrogenation to produce acetaldehyde

$$CH_3CH_2OH \longrightarrow CH_3CHO + H_2$$

is an industrially significant reaction. Although the major current commercial route for acetaldehyde is the Wacker process involving ethylene oxidation, some acetaldehyde is also obtained from the oxidative dehydrogenation of ethanol using a silver catalyst at 480 ºC.

Thus, the vapor phase dehydrogenation of ethanol over a 28% In on porous glass (PG-75) and a 24% Ga/PG-75 was investigated. The results in terms of atomic rate are shown in Figure 13 and are also compared with those of [42] on liquid indium. It is seen again that the rate can be enhanced by several orders of magnitude when the liquid metal catalyst is supported on a porous support, by virtue of the dramatic increase in the active surface area.

5.3 Methycyclohexane Dehydrogenation

The above two examples demonstrate that the rate can be enhanced greatly for reactions previously studied on bulk molten metals. Due to the dramatic increase in the metal surface area, however, it becomes possible to study reactions on supported molten metal catalysts that are too slow to be observed on the limited surface area of liquid metals in the conventional pool reactors (Figure 1). New bifunctional reactions are also feasible in which support plays a supportive catalytic role. Such an example is described here as well as in the next example.

Methylcyclohexane (MCH) dehydrogenation to form toluene, which is a bifunctional reaction, is shown in the following reaction:

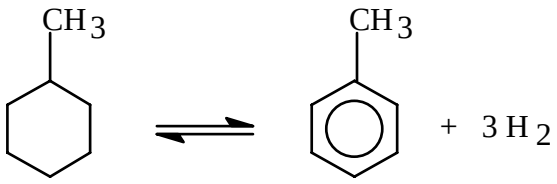

MCH Toluene

This is a very important reaction in catalytic reforming [43], with an estimated 10^8 tons/y of methylcyclohexane being processed in reforming. The resulting production of toluene is accompanied by octane enhancement. MCH has also been suggested as a hydrogen carrier in automotive fuel cell applications [44] as well as an endothermic fuel for hypersonic aircraft [45]. The conventional catalyst for the reaction, Pt/Al_2O_3, for this is initially extremely active, but quickly deactivates due to coking [43]. The reaction is ensemble size insensitive, but coking is ensemble size sensitive. Thus, alloying helps to reduce the deleterious effect of coking. For instance, the bimetallic Pt--Re catalyst on alumina support offers the best combination of initial activity and resistance to deactivation [44]. MCH dehydrogenation on molten metals has not been observed so far due likely to the limited surface area available in pool reactors. Alternatively, this could be due to the bifunctional nature of the catalysis involved in the reaction.

5.3.1 Activity of Various Molten Metals Supported on SiO_2 and γ-Al_2O_3

The activity of different molten metals supported on SiO_2 and γ-Al_2O_3 supports for the conversion of MCH to toluene was compared. Various molten metals such as Sn, Pb, Zn, Cd, In, Te, Bi and Ga were supported via imbibition by mixing 2 g of support powder with 1.8 g of metal catalyst powder in an inert atmosphere and heating above the melting point for 2 hours. The resulting catalyst loading on support was determined gravimetrically. For instance, the loading for Te was found to be 4% molten on alumina. 2.2 g each of the resulting supported catalysts was tested for MCH dehydrogenation under similar conditions at 470 $^{\circ}$C, 10 atm, and a WHSV of 6.3 h^{-1}. As shown in Figure 14(a), most of these metals supported on Al_2O_3 support were found to be active for MCH dehydrogenation, and all possessed high selectivity. In particular, the Zn/Al_2O_3 catalyst exhibited remarkably high catalytic activity. However, none of these catalysts, when tested in bulk (unsupported) form, were found to be active for the dehydrogenation of MCH.

However, all of these catalysts when supported over SiO_2 support, showed relatively low selectivity and activity (Figure 14b). These results indicate that the catalyst support plays an important role for this reaction system. The silica and the alumina supports alone were found to possess little activity for the dehydrogenation of MCH, which clearly, thus, needs a bifunctional catalyst.

Even though Zn showed the highest activity and selectivity for the MCH dehydrogenation reaction, its volatility under reaction conditions could be an issue [Figure 4]. Therefore, Te and Ga SMMC were selected for further investigation of this reaction. Nonetheless, certain alloys were also tested for activity and selectivity, since alloying can, of course, substantially alter the volatility. As shown in Figure 15, many of the alloys possess excellent activity and selectivity for this reaction.

5.3.2 Activity and Stability

MCH dehydrogenation is accompanied by coking and a concomitant decline in activity [43 - 45]. The deactivation and subsequent regeneration of SMM catalysts was, thus, investigated. Thus, a 4% Te/γ-Al_2O_3 SMM catalyst was tested for MCH dehydrogenation as described above at 460 ºC and 10 atm. About 2.4 gm of commercially obtained 1% Pt/γ-Al_2O_3 catalyst (Aldrich) was also tested under similar conditions to directly compare its performance and stability to that of supported molten metal catalyst. The results are summarized in Figure 16. It is evident that the reactivity of the two catalysts is of the same order, which is remarkable since Pt/γ-Al_2O_3 is a very active catalyst for this reaction. For the supported molten metal catalyst, a 25% decline in total conversion of MCH was observed as compared to 75% decline for the 1% Pt/γ- Al_2O_3 catalyst over a 3 h period. Thus, although the initial activity of the commercial Pt catalyst was higher, the eventual activity of the supported molten metal Te catalyst was higher due to the lower susceptibility of the SMM catalyst to deactivation by coking. The final atomic rates calculated for the two catalysts are $r_A = 3.2\text{x}10^{-2}$ molecules/metal atom.s for Pt/γ-Al_2O_3 while $r_A = 2.5\text{x}10^{-3}$ molecules/metal for the Te/γ-Al_2O_3 SMM catalyst.

A coked Ga/γ-Al_2O_3 SMM catalyst was regenerated to study the retention of activity upon regeneration. Thus the coked Ga/γ-Al_2O_3 SMM catalyst was heated in a flow of air to 400 ºC over a period of 1 h and then maintained at that temperature for another 2 hours, in order to burn the coke on the catalyst surface. The regenerated catalyst was then reduced back to metal form in a flow of hydrogen at 650 ºC. The activity of the regenerated catalyst was tested under identical conditions and, as seen in Figure 17, the catalyst was able to largely recover its activity after repeated regenerations. The slight decline in activity could be due to the sintering of the γ-Al_2O_3 support at 650 ºC required to reduce the catalyst to metallic form.

5.3.3 Kinetics over Ga/γ-Al_2O_3 SMMC

A 10% Ga/γ-Al_2O_3 SMM catalyst (Figure 10) was prepared by the solution impregnation method described earlier. The effect of supported catalyst particle size was first studied to determine the influence of diffusional retardation of rate at a temperature of 465 ºC, 1 MPa, and a WHSV of 7.7h^{-1}. It was concluded from these studies that the influence of diffusion is negligible for a particle size smaller than 20-35 mesh. Thus, a particle size of 35-40 mesh was selected for kinetic studies. The stability of the catalyst was next studied. It was found that in the presence of hydrogen the activity of the catalyst did not change significantly within the typical 5 h experimental run indicating little coking. Nonetheless, a fresh catalyst was used for each kinetic run. As shown below, the presence of hydrogen had a negligible effect on the kinetics of the MCH. The MCH dehydrogenation reaction on Ga/γ-Al_2O_3 SMMC under these conditions was found to be extremely clean, with toluene and hydrogen as the only observed products. The experiments were conducted at 435, 450, and 465 ºC, with conversions being kept below 12% in all experiments to validate the basic assumption of differential reactor in kinetic analysis.

Figures 17(a) and 17(b) show the influence of partial pressure of MCH and hydrogen on the initial rate of dehydrogenation of MCH on Ga/γ-Al_2O_3 SMMC at the three different temperatures. The rate increases with MCH partial pressure initially sharply and then more gradually. On the other hand, the hydrogen partial pressure from 2 to 6 atm. showed little influence on the dehydrogenation rate. Lower partial pressures of hydrogen were not utilized to avoid coking of the catalyst.

The expression provided by Nixon [45, 46] for MCH dehydrogenation was tested, i.e.,

$$-r_{MCH} = \left(\frac{k p_{MCH}}{1 + K_{MCH} p_{MCH}}\right)\left(1 - \frac{p_{TOL} p_H^3}{p_{MCH} K}\right) \qquad (8)$$

where, p_{MCH} is MCH partial pressure, p_{TOL} is toluene partial pressure, and p_H is the hydrogen partial pressure, K_{MCH} is the adsorption equilibrium constant of MCH, and K is the thermodynamic equilibrium constant for the overall reaction [18]. Under low conversion, the reverse reaction is negligible, and the (initial) rate of the forward reaction may be rearranged into the form

$$\frac{p_{MCH}}{-r_{MCH,0}} = \frac{1}{k} + \left(\frac{K_{MCH}}{k}\right) p_{MCH} \qquad (9)$$

Thus, the data in Figure 17(a) is plotted in Figure 18 in the manner suggested by this expression, and provides reasonably good linear fits at all three temperatures. Thus, it may be surmised that this is a good model for the MCH dehydrogenation on Ga/γ-Al_2O_3 SMMC. A possible LHHW model corresponding to either the adsorption of MCH or to a surface reaction as the rate limiting step can conform to the zero reaction order for hydrogen along with MCH as the most abundant reactive intermediate on the surface [36] in accordance with these kinetics.

5.4 Selective Catalytic Reduction (SCR) of NO

As a final example, we describe the design of an effective new catalyst for the important case of selective catalytic reduction (SCR) of NO by ethanol in an oxidizing atmosphere and in the presence of water. Reducing NO_x emissions from mobile and stationary combustion sources is an important environmental goal. The catalytic reduction of NO to N_2 by reductants such as hydrocarbons, CO and H_2 is a widely used method for this as, e.g., in the three-way catalytic converters in autos. However, this is effective only in oxygen lean exhausts. When the exhaust contains excess oxygen as, for instance, in most stationary sources and in many vehicles powered with lean-burn gasoline and diesel, the process becomes ineffective, as the reductants preferably react with O_2 rather than with NO. Reductants such as NH_3 that react preferentially with NO are used in stationary sources with catalysts such as platinum, vanadium pentoxide and zeolites. However, the slip of unreacted NH_3 in exhaust is an issue.

Research has, thus, been under way for many years to find viable catalysts for the selective catalytic reduction of NO by hydrocarbons and oxygenated hydrocarbons in oxygen rich exhausts from stationary or mobile combustion sources [47]. A large variety of zeolites has been examined as catalyst candidates for this. However, water vapor, which is inevitably present in the exhaust from combustion sources, substantially inhibits the SCR activity of most zeolite-based catalysts. Further, the hydrothermal stability of zeolites seems to be too low for use in automobile catalytic converters [48]. More recent papers indicate that it is possible to avoid the inhibiting effect of H_2O in the SCR of NO by iso-C_4H_{10} with Fe-ZSM5 [48]. Nevertheless, there is a considerable effort being expended to find active non-zeolitic SCR catalysts that are more active under high temperature steaming conditions.

In this regard, the good water tolerance of various indium-based SCR catalysts has attracted considerable attention. Thus, In, H-ZSM5 has been reported to be a more active catalyst for the SCR of NO by CH_4 in the presence of H_2O than most other catalysts [49]. It was conjectured that the zeolite serves as a bifunctional support for finely dispersed catalytically active In_2O_3 particles in these catalysts [49], where the acidic support purportedly activates CH_4. When In_2O_3 is deposited on supports such as Al_2O_3 [49], its catalytic activity for the SCR of NO by CH_4 diminishes substantially. However, these catalysts show appreciable catalytic activities for the SCR of NO by C_2-C_3 hydrocarbons and alcohols both in the absence and the presence of H_2O [49]. A balance between the indium sites and the acidic sites of γ-Al_2O_3 is needed for adequate SCR reactivity with hydrocarbons [50].

In our effort to find new applications for SMMC, we have observed excellent reactivity for the SCR of NO by alcohols over liquid In catalyst supported on Controlled Pore Glass (CPG) [51]. We thus investigated the effect of H_2, CO, C_3H_8, C_3H_6, CH_3OH, and C_2H_5OH on NO over In-CPG-SMMC in the absence and presence of water vapors [20]. Ethanol was found to be the most active reductant on this catalyst among these. Thus, the proportion of ethanol and oxygen, and the effect of In loading (28 w%, 1.75 w%, 0.95 w% and 0.5 w%) on the reaction were studied at atmospheric pressure in detail in the reaction apparatus described above. To determine whether this new catalyst is competitive with state-of-the-art catalysts reported in the literature, comparative experiments among 28 w% In-CPG-SMMC, H-ZSM-5 and 24 w% In/γ-Al_2O_3 catalysts were also performed with dry as well as wet feed. We also studied the limits of applicability of these catalysts by varying over a wide range the temperature and the gas hourly space velocity (GHSV), and by testing their tolerance towards SO_2 poisoning. To simulate the typical conditions in the catalytic converters for vehicular and stack emissions, all experiments were carried out at high space velocities (GHSV>12,000 h^{-1}) and all SCR experiments were done at GHSV=60,000 h^{-1}. Separate continuous measurements of the nitric oxide and the total NO_x contents in the reactor effluent were made using a Rosemount Model NGA 2000 chemiluminescent NO-NO_x gas analyzer, and were compared with the nitric oxide contents at the reactor inlet to calculate its total conversion. The NO-NO_x detector uses the chemiluminescent method of detection.

5.4.1 SCR Activity of In-CPG-SMMC with Ethanol

Figure 19 (a) compares the catalytic activities of the H-ZSM5 and both the indium based catalysts mentioned above for the SCR of NO in the presence of excess oxygen with ethanol as the reductant, in the absence of water vapors. Both HZSM-5 and the 24 % In/γ-Al_2O_3 catalysts had a higher catalytic activity at temperatures below 500 ºC than the In-CPG-SMMC. However, this latter catalyst surpassed the activity of the other two at temperatures above 500 ºC. The rate of the NO-SCR reaction going through a maximum with rising temperature is a common feature for conventional zeolite and alumina-supported catalysts. At higher temperatures, the competing reactions of direct reductant combustion with oxygen become dominant, i.e., the selectivity of the reaction declines rapidly. The narrow range of temperatures in which these conventional catalysts are active, in fact, constitutes a major impediment for their commercialization. Interestingly, the activity of In-CPG appears to increase monotonically with increasing temperature in the range of temperatures investigated, making it potentially attractive for higher temperatures applications.

Figure 19 (b) compares the activities of the three catalysts when 10 % water is present in the feed, at conditions otherwise identical to those in Figure 19 (a). A comparison to Figure 19 (a) shows that, while water vapors clearly quenched the activity of H-ZSM5 over the entire temperature range, they curiously dramatically enhanced the activity of In-CPG-SMMC. The activity of In/γ-Al_2O_3 was found to be somewhat reduced by the presence of steam. H-ZSM5 and other cation exchanged zeolites have been found to be very sensitive to water vapor. It has been suggested that water competes with NO for adsorption sites, thus lowering the NO surface coverage. It is also conceivable that water moderates the acidity of H-ZSM5 and γ-Al_2O_3, thus reducing activity.

In contrast, water dramatically enhanced the activity of In-CPG-SMMC over the entire temperature range. To the best of our knowledge, thus, In-CPG-SMMC is the most active catalyst for the SCR of NO in the presence of water among the siliceous catalysts available, its activity being comparable, and its hydrothermal stability superior to that of the more conventional catalysts. This activity is probably associated with the acidity of the CPG support in this bifunctional reaction. Infrared spectroscopy shows the presence of surface Si-OH groups together with surface B-OH groups [52], as well as free boron atoms of strong electron-acceptor properties resulting from the residue of B_2O_3 (1-6 %), which remains in the siliceous structure of

CPG after its preparation. Due to the neighboring boron atoms, hydroxyl groups on CPG surface represent strong Brönsted acidic sites, their presence increasing considerably the adsorption properties of CPG compared to silica gel.

The effect of indium loading on reactivity is illustrated in Figure 20 (a). Recall that 28% In loading was calculated as that corresponding to a theoretical monolayer film of liquid indium on CPG. After determining the efficacy of the In-CPG-SMMC for this reaction with a 28% loading, the effect of reduced indium loading was investigated. The reduction of loading dramatically down to 1.75, 0.95, and 0.5 w % In, respectively, in fact, enhanced significantly the NO reduction activity over the entire temperature range. This clearly indicates that the catalyst is bifunctional, although, much as H-ZSM-5, the support itself possesses considerable activity as well. Thus ethanol adsorbs mainly on the acid support sites, while NO and O_2 adsorb almost exclusively on the In sites. The reactions among the species presumably occurs at the interface between the metal and the support sites. Further, around 1% In appears to be around the optimal loading.

Finally, we tested the catalyst resistance to SO_2 poisoning, and the results are shown in Figure 20 (b). The addition of 30 ppm SO_2 (typical amount for automotive exhausts) into the reaction gas mixture caused a slight decrease of NO conversion to N_2 (N_2O). At 500 ^oC, thus, the 0.95 w% In-CPG-SMM catalyst lost 14 % of its initial activity, after 24 hours in the presence of 30 ppm SO_2. However, the NO conversion was restored to about 97 % of the SO_2- free value, when the SO_2 was removed from the feed. Thus, SO_2 is a reversible reaction inhibitor and not an irreversible catalyst poison.

It is, further, significant that In-CPG-SMMC seems to have no aging problems since the catalytic performance remains intact when catalytic tests were carried out at different reaction conditions for more than two weeks.

6 Conclusions

Development of a novel class of heterogeneous catalysts, namely supported molten metal catalysts, or SMMC, is described in which catalytic metals or alloys that are molten under reaction conditions are utilized effectively for catalytic reactions by dispersing them as nano- or micro-droplets on the pore surface of conventional porous supports. This allows much greater utilization of the liquid metal than is possible in conventional gas-liquid contactors, while

eliminating the corrosion concerns associated with the use of molten metals. It is shown that this technique can increase the rate of a reaction by several orders of magnitude due to increased catalyst dispersion and the corresponding increase in surface area. Thus, the technique allows for the possibility of utilizing molten metals for reactions for which in sufficient reactivity was found in conventional reactors. Furthermore, the technique also allows the development of bifunctional catalysts, where the support is also actively engaged in the reaction mechanism.

The possible metal candidates for the supported molten metal technique lie in groups 1, 12, 13, 14, 15, and 16 of the periodic table based on their relatively low melting points. The choice of the support is based on their surface area, porosity and pore size distribution, inertness with respect to the molten metal, bifunctionality, mechanical strength, and the wetting characteristics of the support by the molten metal. In addition to the conventional precursor solution impregnation method, SMMC can also be easily prepared using the vapor deposition method or the direct imbibition method. The SMM catalysts were characterized by BET surface area, pore volume, pore size distribution, and dispersion measurements, as well as by scanning electron microscopy (SEM) and transmission electron microscopy (TEM).

While the SMMC technique could potentially be applied to a wide variety of catalytic reactions, the reactions investigated here included 1) those that have been previously studied on molten metal in pool reactors to determine the enhancement in rate afforded by the increased dispersion, and 2) new reactions which could not have been observed in conventional pool reactors due to the very low active area available or those that are bifunctional in nature. Examples of the first type include dehydrogenation of tetralin and ethanol, which conclusively demonstrate the dramatic enhancement in reaction rate possible as a result of increased dispersion and surface area in SMMC. Examples of the second type include methycyclohexane (MCH) dehydrogenation and selective catalytic reduction (SCR) of NO with ethanol. Both of the latter are of potential practical significance. The MCH dehydrogenation catalyst to produce toluene is active and more stable than the conventional Pt-based catalyst, while the catalyst for the SCR of NO with ethanol appears superior to existing catalysts in terms of water tolerance, activity, and range and temperatures.

A wide variety of molten metal and alloy catalysts supported on γ-Al_2O_3 showed good activity and excellent selectivity for the MCH dehydrogenation. Of these Te/γ-Al_2O_3 and Ga/γ-Al_2O_3 bifunctional catalysts were investigated in more detail, including kinetics. The In-CPG-

SMMC is a new catalyst that shows several distinct properties as compared to those of other SCR catalysts including other In-based catalysts. Of the various reductants investigated ethanol was the most effective. The activity of this new catalyst appears to increase monotonically with temperature. This feature makes In-CPG-SMMC attractive for practical applications at temperatures above 500 ^{o}C for the SCR of NO in exhaust streams containing water and excess oxygen. Even though in a dry feed the catalytic activity of H-ZSM-5 is superior to that of In-CPG-SMMC, 10 % water substantially enhanced the performance of this new catalyst, while inhibiting the activity of both H-ZSM-5 and In/γ-Al_2O_3 over the entire temperature range studied. The optimum loading of In is around 1%, and the catalyst is bifunctional. Ethanol adsorbs only on the acid support sites, while NO and O_2 adsorb on the metal sites, with the reactions among these species occurring at the interface between metal and support.

In summary, a new class of heterogeneous catalysts has been developed that provides new options to design catalysts with materials that were so far unavailable to the catalyst engineer.

7 Acknowledgement

We gratefully acknowledge the financial support provided by DOE for this work through Grants DE-FG02-96ER12184 and DE-FG26-97FT97268.

8 References

[1] Ertl, G., Knözinger, H., and Weitkamp, J., eds., *Handbook of Heterogeneous Catalysis*, 5 volumes, Wiley-VCH, New York, 1997.

[2] Bell, A. T., "The Impact of Nanoscience on Heterogeneous Catalysis," *Science*, **229**, 1688-1691 (2003).

[3] Somorjai, G. A., and Rioux, R. M., "High Technology Catalysts toward 100% Selectivity. Fabrication, Characterization, and Reaction Studies," *Catalysis Today*, **100**, 201-215 (2005).

[4] Parshall, G. W., *Homogeneous Catalysis*, John Wiley, New York (1980).

[5] Cole-Hamilton, D. J., "Homogeneous Catalysis – New Approaches to Catalyst Separation, Recovery, and Recycling," *Science*, **229**, 1702-1706 (2003).

[6] Hartley, F. R., "*Supported Metal Complexes"*, D. Reidel Pub-Co, Dordrecht, Holland, 1985.

[7] Raje, A. P., and R. Datta, "Activity and Stability of Ion-Exchange Resin Supported Tetrakis (Triethyl Phosphite) Nickel Hydride Catalyst. Vapor Phase Isomerization of *n*-Butene," *J. Mol. Catal.*, **72**, 97, 1992.

[8] Rony, P. R., "Supported Liquid-Phase Catalysts," *Chem. Engng. Sci.*, **23**, 1021, 1968.

[9] Datta, R., and R. G. Rinker, "Supported Liquid-Phase Catalysis: I. A Theoretical Model for Transport and Reaction," *J. Catal.*, **95**, 181, 1985a.

[10] Datta, R.; Savage, W., and R. G. Rinker, "Supported Liquid-Phase Catalysis: II. Experimental Evaluation of the Flux Model for Liquid-Loaded Porous Media," *J. Catal.*, **95**, 193, 1985b.

[11] Datta, R., Rydant, J. J., and R. G. Rinker, "Supported Liquid-Phase Catalysis: III. Experimental Evaluation of the Diffusion-Reaction Model," *J. Catal.*, **95**, 202, 1985c.

[12] Lerou, J. J., and Reilly, C. R., "Supported Liquid Phase Catalysis in Selective Oxidation," *Catalysis Today*, **41**, 433-441 (1998).

[13] Arhancet, J. P., Davis, M. E., Merola, J. S., and Hanson, B. E., "Hydroformylation by Supported Aqueous-Phase Catalysis: A New Class of Heterogeneous Catalysts," *Nature* **339**, 454 - 455 (1989).

[14] Parida, S., Datta, R., and Dordick, J. S., "Supported Aqueous-Phase Enzyme Catalysis in Organic Media," *Appl. Biochem. and Biotech.*, **33**, 1-14 (1992).

[15] Rao, V., and R. Datta, "Development of a Supported Molten-Salt Wacker Catalyst for the Oxidation of Ethylene to Acetaldehyde," *J. Catal.*, **114**, 337 (1988).

[16] Datta, R., and D. P. Eyman, "Catalyst Dispersed in Supported Molten Salt," U. S. Patent No. 4,898,845, Feb. 6, 1990.

[17] Mehnert, C. P., "Supported Ionic Liquid Catalysis," *Chem. Eur. J.*, **11**, 50-56 (2005).

[18] Singh, A., "Design and Development of Supported Molten Metal Catalysts (SMMC)," Ph.D. Thesis, The University of Iowa, Iowa City, IA (1998).

[19] Datta, R., Singh, A., Halasz, I., and Serban, M., "Supported Molten-Metal Catalysts," U.S. Patent No. 6,218,326 B1, Apr. 17, 2001.

[20] Serban, M., "Selective Catalytic Reduction of Nitrogen Oxide Over Supported Molten Metal Catalysts," Ph.D. Thesis, Worcester Polytechnic Institute, Worcester, MA (2001).

[21] Ogino, Y., *Catalysis and Surface Properties of Liquid Metals and Alloys*, Marcel Dekker, Inc, New York, 1987.

[22] Ipatiew, W., *Ber.*, **34**, 1047, 3579, (1901).

[23] Steacie, E. W. R., and Elkin, E. M., "A Comparison of the Catalytic Activity of Liquid and Solid Surfaces. The Decomposition of Methanol on Solid and Liquid Zinc, *Proc. Roy. Soc. London*, A142, 457 (1933).

[24] Hartman, R. J., and Brown, O. W., "Catalytic Activity of Cadmium," *J. Phys. Chem.*, **34**, 2651 (1930).

[25] Adadurow, I. E., and Didenko, P. D., "Catalysis by Fusion," *J. Am. Chem. Soc.*, **57**, 2718 (1935).

[26] Friedman, S., Kaufman, M. L., and Wender, I., "Alkali Metals as Hydrogenation Catalysts for Aromatic Molecules, *J. Org. Chem.*, **36**, No.5, 694 (1971).

[27] Masel, R. I., *Principles of Adsorption and Reaction on Solid Surfaces*, John Wiley, New York (1996).

[28] Bligaard, T., Norskov, J. K., Dahl, S., Matthiesen, J., Christensen, C. H., and Sehested, J., "The Bronsted-Evans-Polanyi Relation and the Volcano Curve in Heterogeneous Catalysis," *J. Catal.*, **224**, 206-217 (2004).

[29] Nilsson, A., Pettersson, L. G. M., Hammer, B., Bligaard, T., Christensen, C. H., and Norskov, J. K., "The Electronic Structure Effect in Heterogeneous Catalysis," *Catal. Lett*., **100**, 111-114 (2005).

[30] Somorjai, G. A., McCrea, K. R., and Zhu, J., "Active Sites in Heterogeneous Catalysis: Development of Molecular Concepts and Future Challenges," *Topics Catal*., 18, 157-166 (2002).

[31] Iida, T., and Guthrie, R. I. L., *The Physical Properties of Liquid Metals*, Clarendon Press, Oxford (1988).

[32] Lide, D., Editor-in-Chief, *CRC Handbook of Chemistry and Physics*, 73rd Ed., CRC Press (1992).

[33] Richardson, J. T., *Principles of Catalyst Development*, Plenum, New York (1989).

[34] Sangiorgi, R., Muolo, M. L., Chatain, D., and Eustathopoulos, N., *J. Am. Ceram. Soc*., 71, 742 (1988).

[35] Gregg, S. J., and Sing, K. S. N., *Adsorption, Surface Area and Porosity*, 2nd Ed., Academic Press, New York (1997).

[36] Boudart, M., and Djéga-Mariadassou, G., *Kinetics of Heterogeneous Catalytic Reactions*, Princeton University Press, New Jersey (1984).

[37] Zeldowitsh, J., "On the Theory of the Freundlich Adsorption Isotherm," *Acta Physicochimica U.S.S.R.*, Vol.1, No.6, p.9, (1935).

[38] Ghandi, H. S., and Shelef, M., "The Adsorption of Nitric Oxide and Carbon Monoxide on Nickel Oxide, *J. Catal.*, **24**, 241, (1972).

[39] Takahashi, K., and Y. Ogino, "Liquid Tellurium as a Catalyst for the Dehydrogenation of Several Polynuclear Hydrocarbons," *Chem. Lett*., **???,** 423 (1978).

[40] Takahashi, K., and Y. Ogino, "Studies on the Catalysis of Molten Metal 13. Kinetics of Dehydrogenation of Tetralin Over Molten Tellurium Catalyst," *Fuel*, **60**, 975 (1981).

[41] Somorjai, G. A., *Introduction to Surface Chemistry and Catalysis*, John Wiley, New York, 1994.

[42] Saito, Y., Hiramatsu, N., Kawanami, N., and Ogino, Y., *Bull. Jap. Petrol. Inst*., **14**, 169 (1972).

[43] Beltramini, J. N., Wessel, T. J., and Datta, R., "Kinetics of Deactivation of Bifunctional Pt/Al_2O_3-Cl Catalysts by Coking during Methylcyclopentane Reforming," *AIChE Journal*, **37**, 845-854 (1991).

[44] Jothimurugesan, K.; Bhatia, S., and R. D. Srivastava, "Kinetics of Dehydrogenation of Methylcyclohexane over a Platinum-Rhenium-Alumina catalyst in the Presence of Added Hydrogen," *Ind. Eng. Chem. Fundam.*, **24**, 433, (1985).

[45] Nixon, A. C., A *Study of Endothermic and High Energy Fuels for Airbreathing Engines* (1986).

[46] Sinfelt, J.H.; Hurwitz, and R.A. Sulman, "Kinetics of Methylcyclohexane Dehydrogenation Over Pt-Alumina," *J. Phys. Chem.*, **64**, 1559 (1960).

[47] Armor, J. N., "Environmental Catalysis, Review," *Appl. Catal. B: Env.*, **1**, 221 (1992).

[48] Feng, X., and Hall, W. K., "Fe-ZSM-5: A Durable SCR Catalyst for NO Removal from Combustion Sources," *J. Catal.*, **166**, 368 (1997).

[49] Zhou, X., Zhang, T., Xu, Z., and Lin, L., "Selective Catalytic Reduction of Nitrogen Monoxide with CH_4 over Impregnated In/ZSM-5 in the Presence of Excess Oxygen," *Catal. Lett.*, **40**, 35 (1996).

[50] Gervasini, A., Perdigon-Melon, J. A., Guimon, C., and Auroux, A., "An In-depth Study of Supported In_2O_3 Catalysts for the Selective Catalytic Reduction of NO_x: The Influence of the Oxide Support," *J. Phys. Chem. B*, **110**, 240-249 (2006).

[51] Serban, M., Halasz, I., and Datta, R., "New Water Tolerant Supported Molten Indium Catalysts for the SCR of NO by Ethanol," *Catal. Lett.*, **63**, 217 (1999).

[52] Dawidowicz, A. L., "Controlled Porosity Glasses (CPGs) as Adsorbents, Molecular Sieves, Ion-Exchangers and Support Materials," in *Adsorption on new and Modified Inorganic Sorbents*, *Studies in Surface Science and Catalysis*, Eds. Dabrowski, A., Terykh, V.A., Elsevier, p. 31, (1996).

Table 1. Some of the Possible Molten Metal Catalysts Suitable for SMMC System

Metals	Melting Point (ºC)	Boiling Point (ºC)
Hg	-38.9	357
Ga	29.8	1700
Na	97.5	800
In	155	1450
Li	186	1336
Se	217	649
Sn	232	2260
Bi	271	1450
Tl	303	1650
Cd	321	767
Pb	327	1620
Zn	419	907
Te	449.5	989.8
Sb	631	1380
Mg	651	1110
Al	660	2057

Table 2. Some Possible Metal Alloys Suitable for SMMC System [24].

Alloy	**Composition (Wt.%)**	**Melting Point (^{o}C)**
Cs-Rb	87:13	-40
Cs-Na	95:5	-30
K-Na	78:22	-11
Rb-Na	92:8	-8
Ga-In-Sn	65.5:21.5:16.0	10.7
Ga-Sn-Zn	82:12:6	17
Na-K	40:60	27
Rb-K	68:32	33
In-Bi-Sn	51:32.5:16.5	60.5
Na-Rb	60:40	67
In-Sn	49:51	120
In-Cd	75:25	120
Bi-Sn-Pb	46.1:34.2:19.7	123
Bi-Pb	55.5:44.5	124
Bi-Sn-Zn	56:40:4	130
Bi-Sn	58:42	140
Bi-Cd	60:40	140
Sn-Pb	38:62	183
Tl-Bi	52:48	185
Sn-Pb	70:30	192
Sn-Zn	92:8	199
Sn-Cu	99.25:0.75	227
Na-In	20:80	267
Na-Pb	30:70	386

Table 3. Different Types of Catalyst Supports (Richardson, 1989).

Type	**Nature**	**Examples**	**M.P. (^oC)**	**Remarks**
1.Oxides	Inert	$MgAl_2O_4$	2408	Multimetallic oxides have spinel structure and are very stable
		$MgCr_2O_4$	2300	
		$ZnCr_2O_4$	2173	
		$ZnAl_2O_4$	2100	
		$CaSiO_3$	1813	
		Honeycomb		Honeycomb and foam ceramics (wash coated) have low pressure drops.
		Foam Ceramics		
	Amphoteric	ThO_2	2323	
		ZrO_2	2988	ZrO_2 is stable at high temperatures
		CeO_2	2873	
		Cr_2O_3	2708	Cr_2O_3 causes dehydration
		La_2O_3	2588	
		α-Al_2O_3	2318	α-Al_2O_3 has low surface area
		TiO_2	2113	
	Acidic	γ-Al_2O_3	2318	γ-Al_2O_3 is most common support. Unstable under acidic conditions.
		SiO_2	1973	
		SiO_2-Al_2O_3	1818	SiO_2 is stable. Includes silica gel, kieselguhr, etc.
		Zeolites		
		Pillared Clays		
		ZrO_2		
		Stabilized Al_2O_3		
	Basic	MgO		
		CaO	3073	Magnesia has poor strength.
		Ca_2SiO_4	2853	
		BaO	2407	
		Ca_3SiO_5	2196	
			2173	
2.Other		Carbon		
		Carbides		
		Nitrides		Carbon has limited stability. Carbides are inert.
		Carbonates		
		Sulfates		
		Phosphates		Carbonates, sulfates, and phosphates lack stability.

Table 4. Effect of Metal Loading on the Specific Surface Area (SA) and Pore Volume (PV) on In-CPG-SMMC Samples.

Catalyst	**SA_{BET} (m^2/g)**	**PV (cm^3/g)**	**ΔPV (cm^3)**	**V_{In} (cm^3)**
Controlled Pore Glass	171	0.565	---	---
1.75w% In-CPG-SMMC	158	0.540	0.025	0.0024
7 w% In-CPG-SMMC	151	0.531	0.034	0.0096
14 w% In-CPG-SMMC	143	0.505	0.026	0.0192
28 w% In-CPG-SMMC	138	0.471	0.034	0.0280

Note:

ΔPV = Change in Pore Volume

V_{In} = Volume of Added Metal (Compared to the Previous Loading).

Figure Captions

Figure 1. Reactors Used for Studying Molten Metal Catalysts: (a) Bubbling Type Reactor; and (b) Tubular Duct Reactor.

Figure 2. Schematic of a Supported Molten Metal Catalyst (SMMC): (a) nano-droplets for nonwetting melts; (b) nano-films for wetting melts; and (c) films for wetting melts at higher loadings.

Figure 3. Possible Metal Candidates for the SMMC.

Figure 4. Vapor Pressures of Liquid Metals [23].

Figure 5. Transparent Pyrex Furnace for Visually Inspecting the Interaction of Supports and Molten Metals in an Air Free Environment at Elevated Temperatures.

Figure 6. Schematic of a High Vacuum/High Pressure Catalytic System.

Figure 7. (a) Nitrogen Adsorption Isotherms at 77 K for the 28 w% In-CPG-SMMC. (b) BET Plot for the 28 w% In-CPG-SMMC.

Figure 8. Pore Size Distribution of Different Samples of In-CPG-SMMC.

Figure 9. (a) Oxygen Chemisorption Isotherms for the 1.75 w% In-CPG-SMMC at Different Temperatures. (b) Linearized Plots of the Freundlich Equation for the Oxygen Chemisorption Isotherms for the 1.75 w% In-CPG-SMMC.

Figure 10. (a) SEM Picture of 28 w% In-CPG-SMMC, X7000 Magnification, V_{acc} = 5 kV. Indium is Visible as Micro-Droplets of Diameter < 1.4 μm. (b) Transmission electron micrograph of 10% Ga/γ-Al_2O_3 catalyst showing Ga particles < 20 nm.

Figure 11. Calculated turnover number (N_T) (or turnover frequency, TOF) for tetralin dehydrogenation reaction over molten Te catalyst in a duct reactor [40].

Figure 12. Comparison of atomic rates of dehydrogenation of tetralin over 2 grams of 3% Te/γ-Al_2O_3 catalyst and 70 grams of unsupported molten Te catalyst [39] at 1 atm. And 0.057 mol/h flowrate of tetralin.

Figure 13. Comparison of the atomic rate of dehydrogenation of ethanol over a 28% In on porous glass (PG-75), a 24% Ga/PG-75 and liquid indium [42].

Figure 14. Comparison of the activity and selectivity of different molten metals supported on (a) γ-Al_2O_3 and (b) SiO_2 supports for the dehydrogenation of MCH to toluene at 470 ºC, 1 MPa, and a WHSV = 6.3 h^{-1}.

Figure 15. Comparison of the activity and selectivity of different molten metal alloys supported on γ-Al_2O_3 for the dehydrogenation of MCH to toluene at 470 ºC, 1 MPa, and a WHSV = 6.3 h^{-1}.

Figure 16. (a) Comparison of the activity and stability of commercial 1% Pt/γ-Al_2O_3 and 4% Te/γ-Al_2O_3 SMM catalyst or the dehydrogenation of MCH to toluene at 460 ºC, 1 MPa, and a WHSV = 13.8 h^{-1}. (b) Effect of catalyst regeneration for Te/γ-Al_2O_3 SMM catalyst on the rate of MCh dehydrogenation at 460 ºC, 1 MPa, and a WHSV = 7.7 h^{-1}.

Figure 17. The influence of partial pressure of MCH (a) and hydrogen (b) on the initial (low conversion) rate of dehydrogenation of MCH on Ga/γ-Al_2O_3 SMMC at the three different temperatures.

Figure 18. The data for dehydrogenation of MCH on Ga/γ-Al_2O_3 SMMC in Figure 17(a) is plotted in the manner suggested by Eq. (9).

Figure 19. Total NO Conversion (solid lines) and Conversion to N_2 (dashed lines) for 1000 ppm NO, 5 % O_2, 0.65 % C_2H_5OH, Balance He, GHSV = 60,000 h^{-1} over H-ZSM5 (❍), 24 % In/γ-Al_2O_3 (■), and 28 % In-CPG-SMMC (◊) (a) under Dry Conditions and (b) in the Presence of 10 % H_2O.

Figure 20. (a) Effect of In Loading on the Conversion of NO to N_2 (N_2O) over In-CPG-SMMC. Reactants: 1000 ppm NO + 5 % O_2 + 0.65 % C_2H_5OH, Balance He, GHSV = 60,000 h^{-1}. ◊: 28 w% In, ❍: 1.75 w% In, ■: 0.95 w% In, ●: 0.5 w% In and ♦: CPG. (b) Effect of SO_2 on the NO Conversion to N_2 (N_2O) over 0.95 % In-CPG- SMMC. Conditions similar to (a) with 30 ppm SO_2.

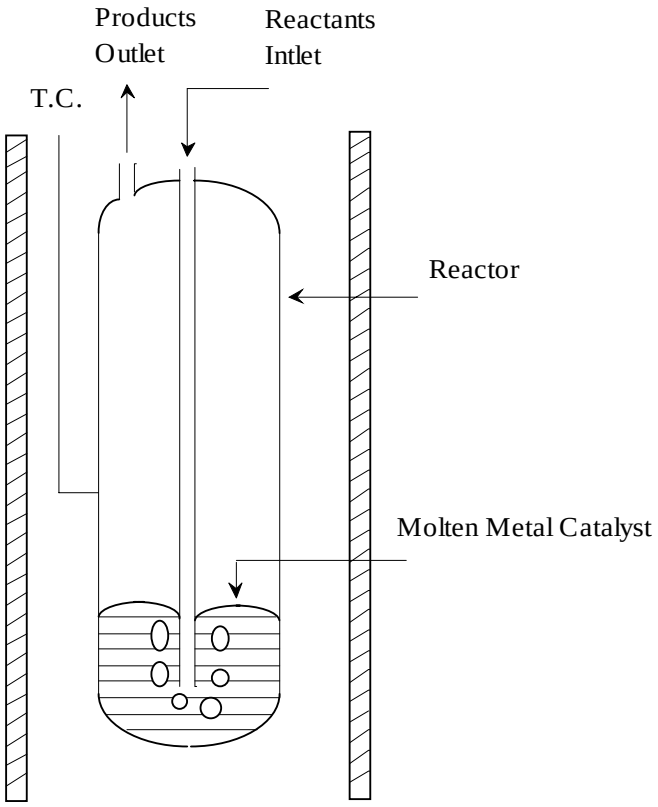
Products
Outlet
Reactants
Intlet
T.C.
Reactor
Molten Metal Catalyst

(a)

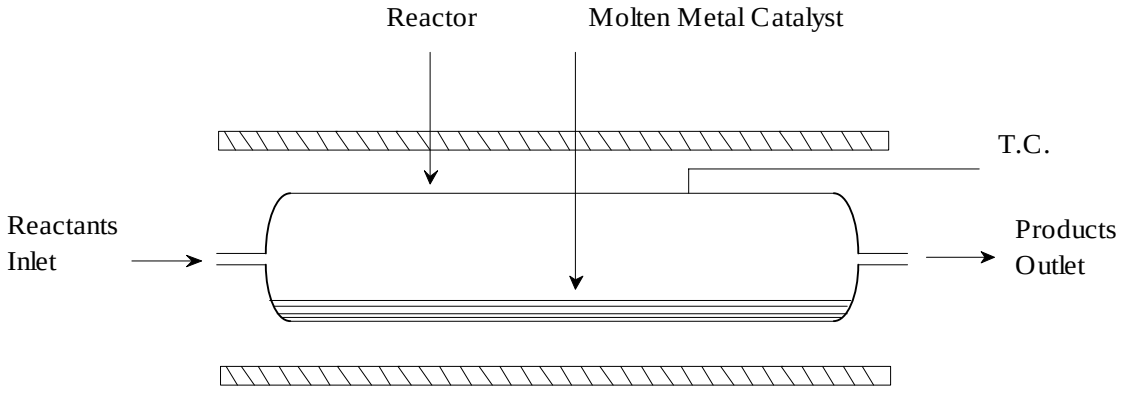
Reactor
Molten Metal Catalyst
T.C.
Reactants
Inlet
Products
Outlet

(b)

Figure 1

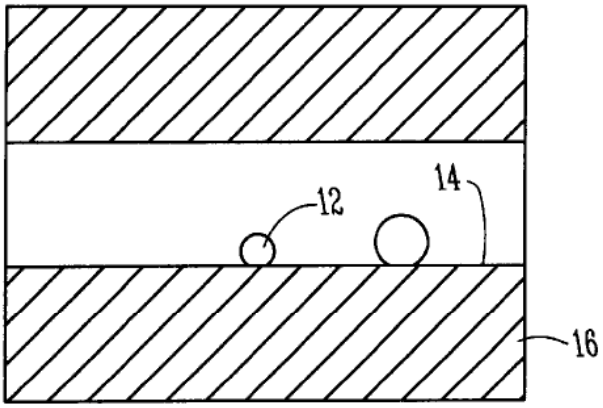

(a)

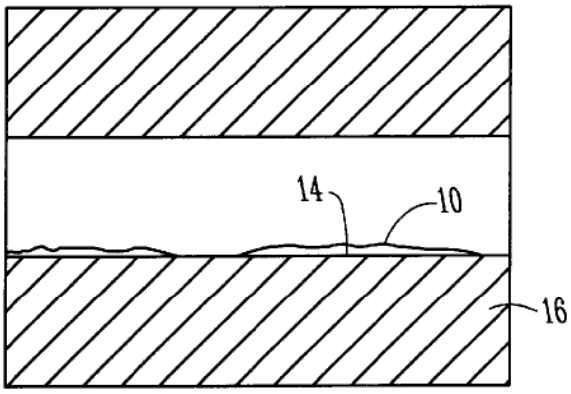

(b)

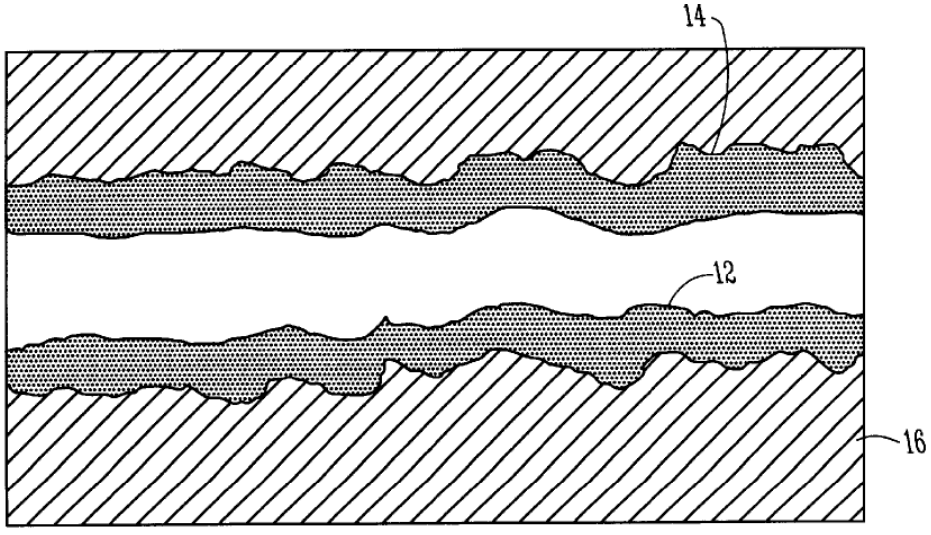

(c)

Figure 2

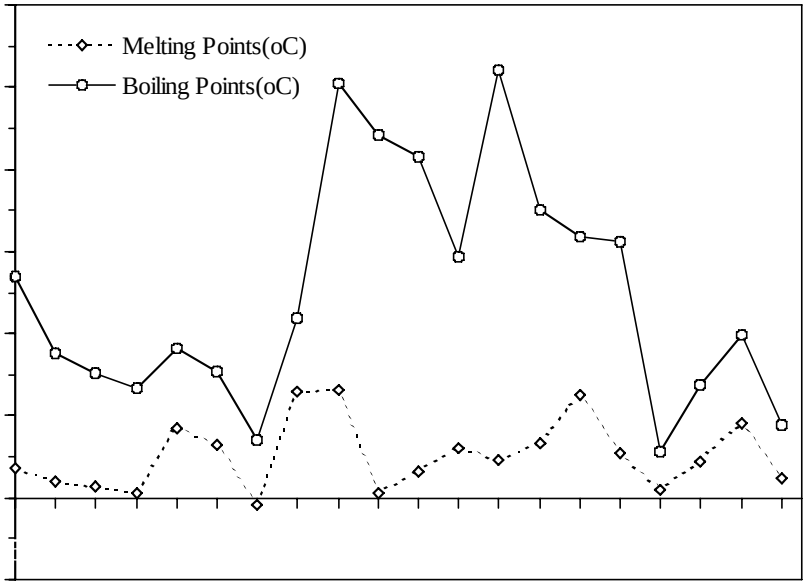
Melting Points(oC)
Boiling Points(oC)

(a)

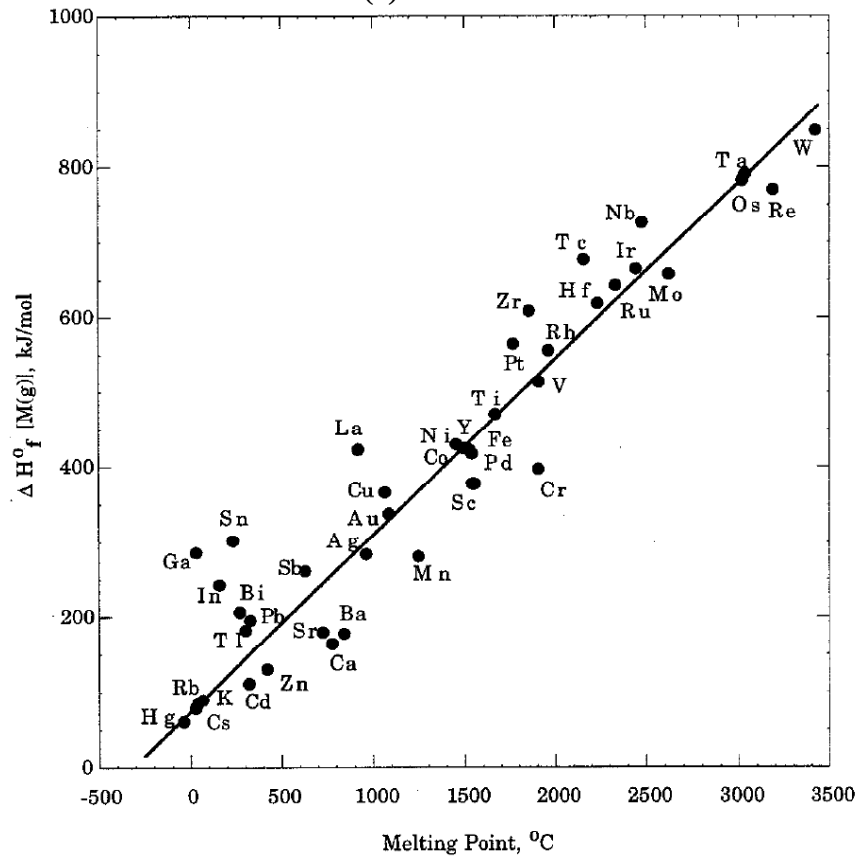
1000
800
600
400
200
0
-500
0
500
1000
1500
2000
2500
3000
3500
Melting Point, °C
ΔH°f [M(g)], kJ/mol
W
Ta
Os
Re
Nb
Tc
Ir
Hf
Mo
Ru
Zr
Rh
Pt
V
Ti
La
Ni
Y
Fe
Co
Pd
Cr
Cu
Sc
Au
Ag
Mn
Sn
Ga
Sb
In
Bi
Pb
Ba
Sr
Tl
Ca
Zn
Rb
K
Cd
Hg
Cs

(b)

Figure 3

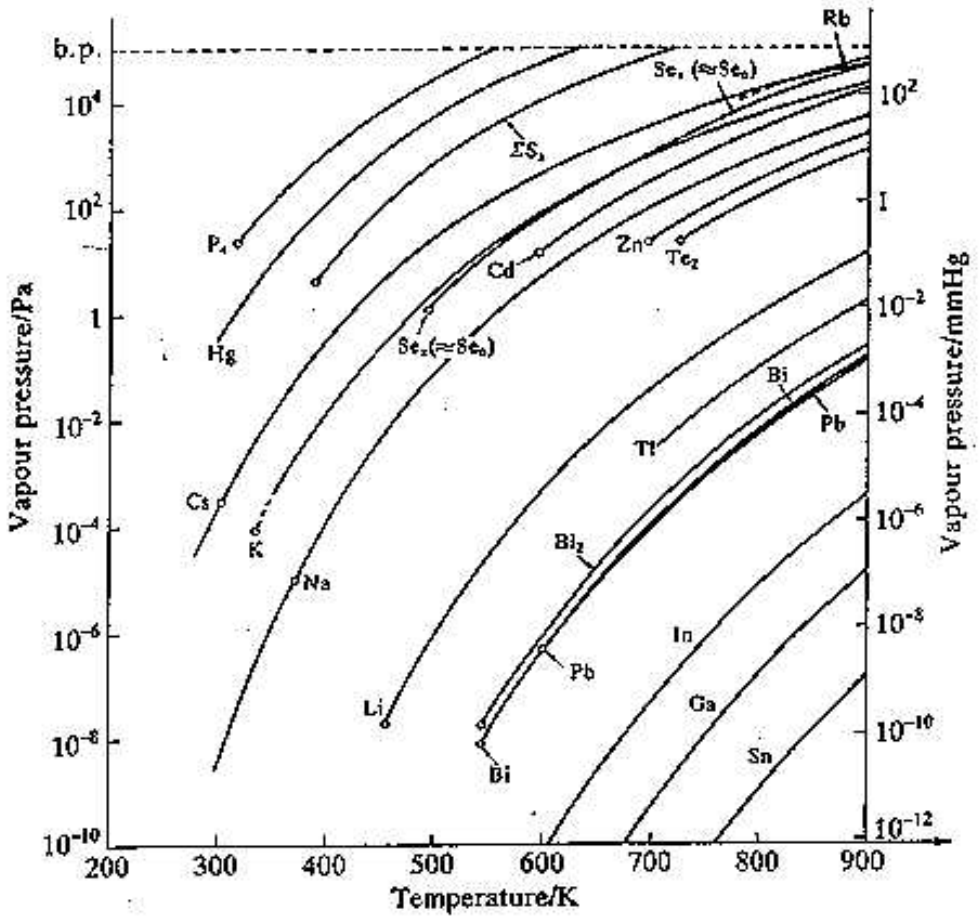
b.p.
Rb
Se, (≈Se6)
ΣS2
P4
Hg
Cd
Zn
Te2
Se2(≈Se6)
Cs
K
Na
Li
Tl
Bi
Pb
Bi2
Pb
In
Ga
Sn
Bi
Vapour pressure/Pa
Vapour pressure/mmHg
Temperature/K
10^4
10^2
1
10^-2
10^-4
10^-6
10^-8
10^-10
10^2
1
10^-2
10^-4
10^-6
10^-8
10^-10
10^-12
200
300
400
500
600
700
800
900

Figure 4

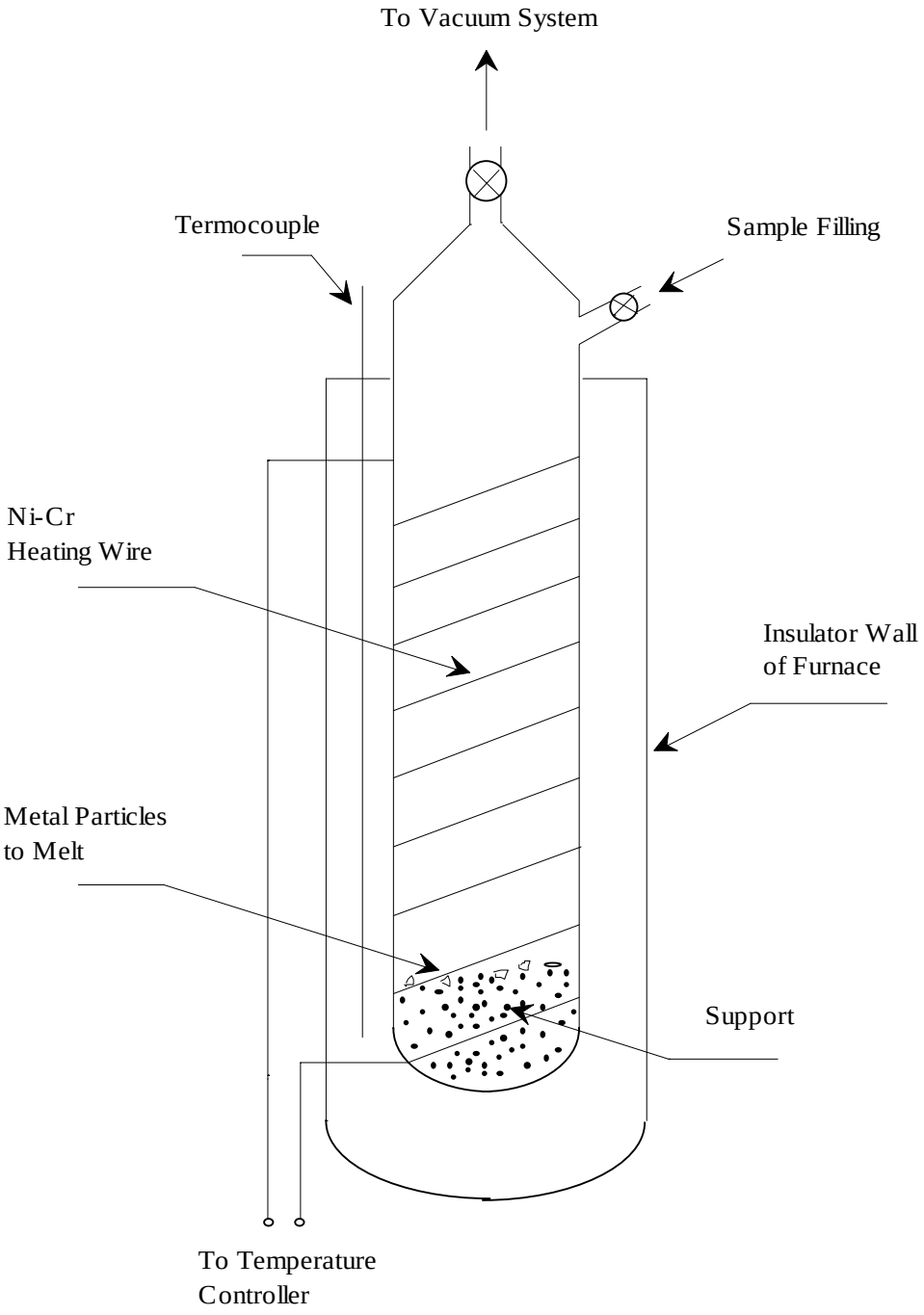
To Vacuum System
Termocouple
Sample Filling
Ni-Cr
Heating Wire
Insulator Wall
of Furnace
Metal Particles
to Melt
Support
To Temperature
Controller

Figure 5

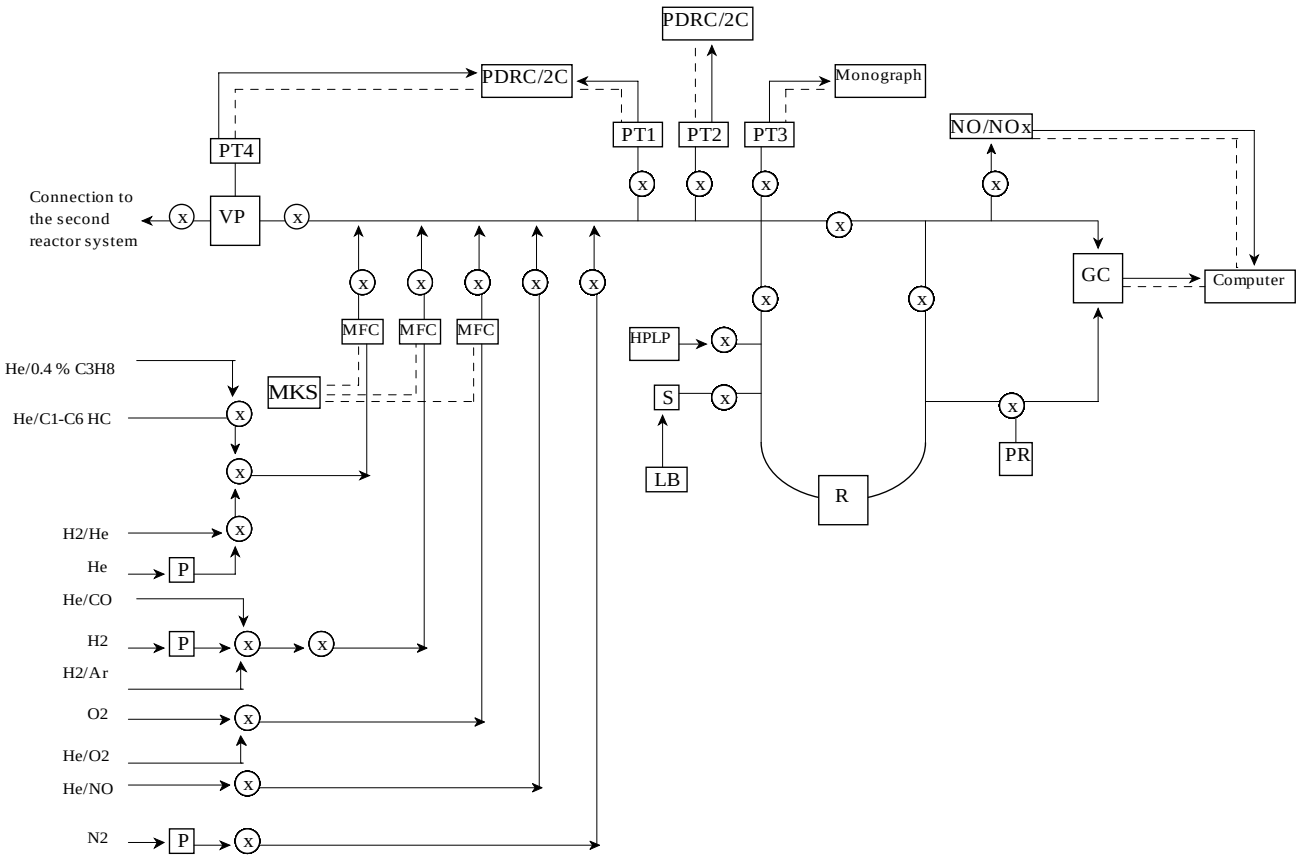

Legend for Figure 6

VP	Alcatel Model Drytel Micro Ceramic Roughing and Molecular Drag Vacuum Pump
MFC	MKS Type 1179 Mass Flow Controllers
PT1	Baratron Type 128A Pressure Transducer (range 10^{3}-10^{-1} Torr)
PT2	Baratron Type 128A Pressure Transducer (range 10^{2}-10^{-2} Torr)
PT3	Omega Model PX-931 Pressure Transducer
PT4	Baratron Type 128A Pressure Transducer (range 10^{-1}-10^{-5} Torr)
P	Oxy-Purge Purifier
HPLP	Gilson High Pressure Liquid Pump Model 302 (0.01-5 ml/h)
R	Catalytic Reactor for Kinetic Measurements at High and Low Pressures
PR	Swagelok High Temperature Pressure-Regulator Microvalve
GC	Gas Chromatograph Model 8610 with TCD and FID Detectors
NO/NO_x	Chemiluminescent NO/NO_x Analyzer
S	Stainless Steel Saturator
LB	Fisher Scientific Liquid Bath
MKS	MKS Model 247C 4 Channel Power Supply/Readout
PDRC/1C	MKS 1 Channel Power Supply/Readout
PDRC/2C	MKS 1 Channel Power Supply/Readout
Monograph	Omega Digital Pressure Gauge

Figure 6

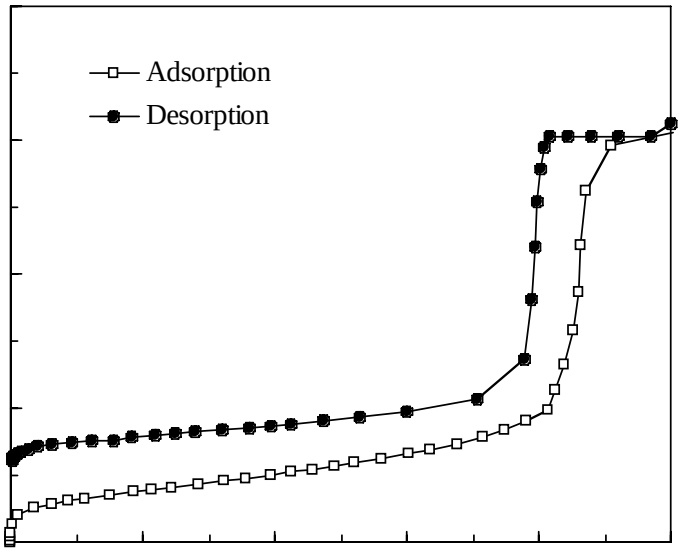

(a)

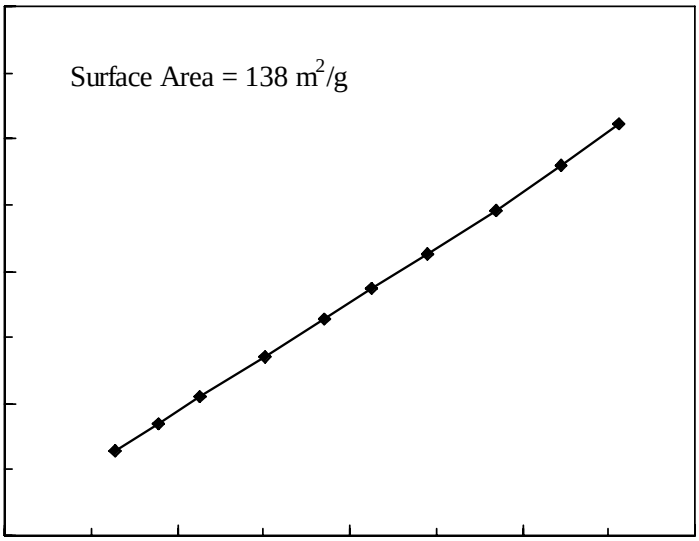

(b)

Figure 7

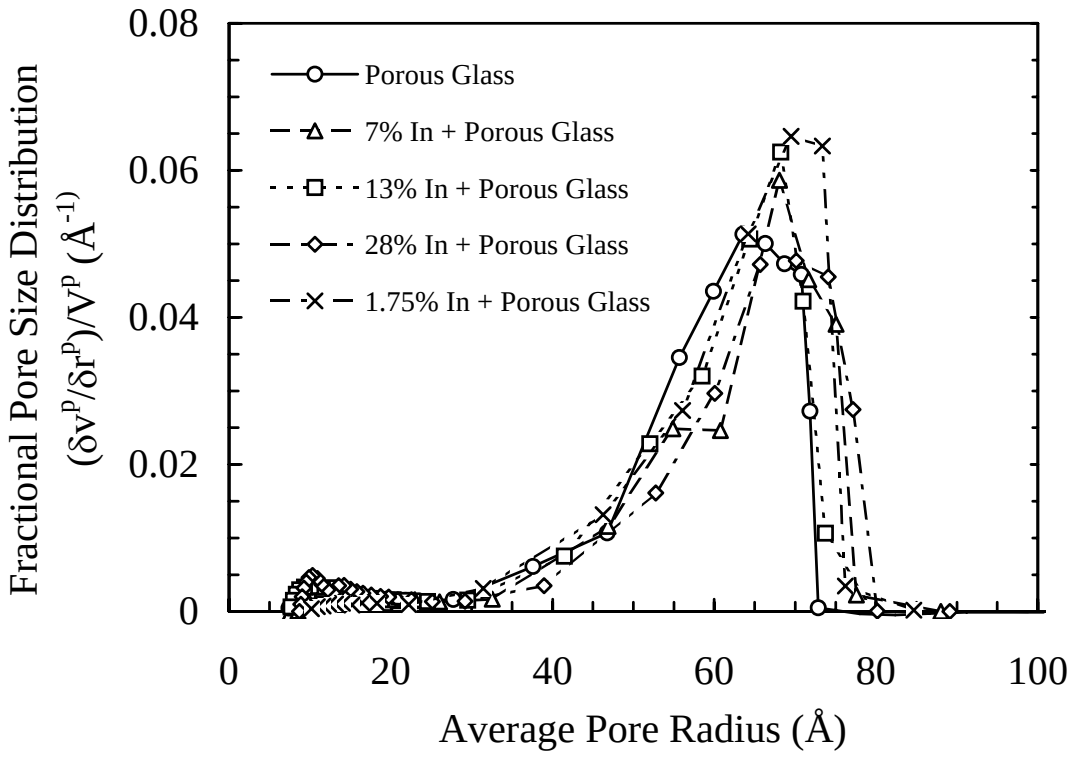
0.08
0.06
0.04
0.02
0
0
20
40
60
80
100
Fractional Pore Size Distribution
$(\delta v^p/\delta r^p)/V^p$ (Å^{-1})
Average Pore Radius (Å)
Porous Glass
7% In + Porous Glass
13% In + Porous Glass
28% In + Porous Glass
1.75% In + Porous Glass

Figure 8

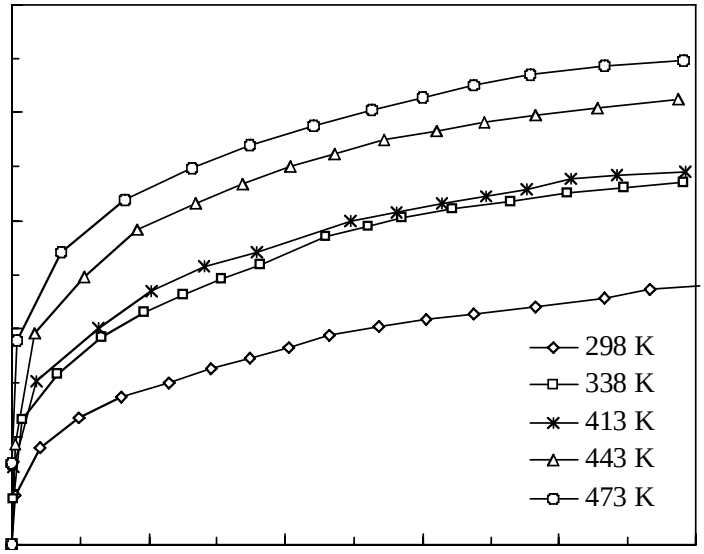

(a)

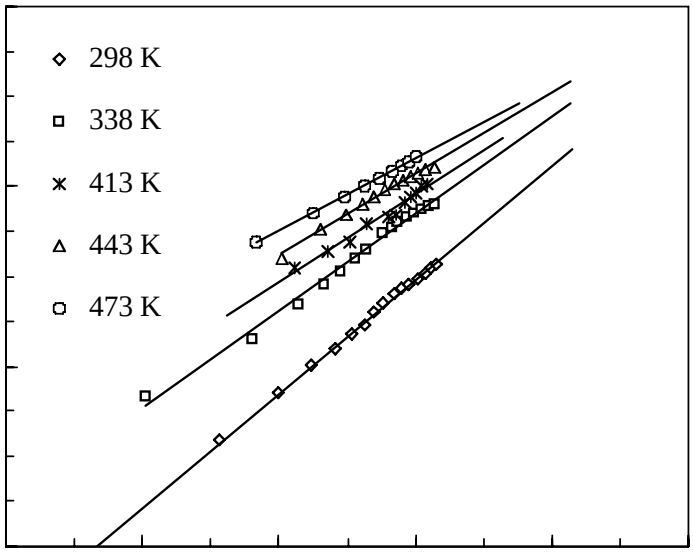

(b)

Figure 9

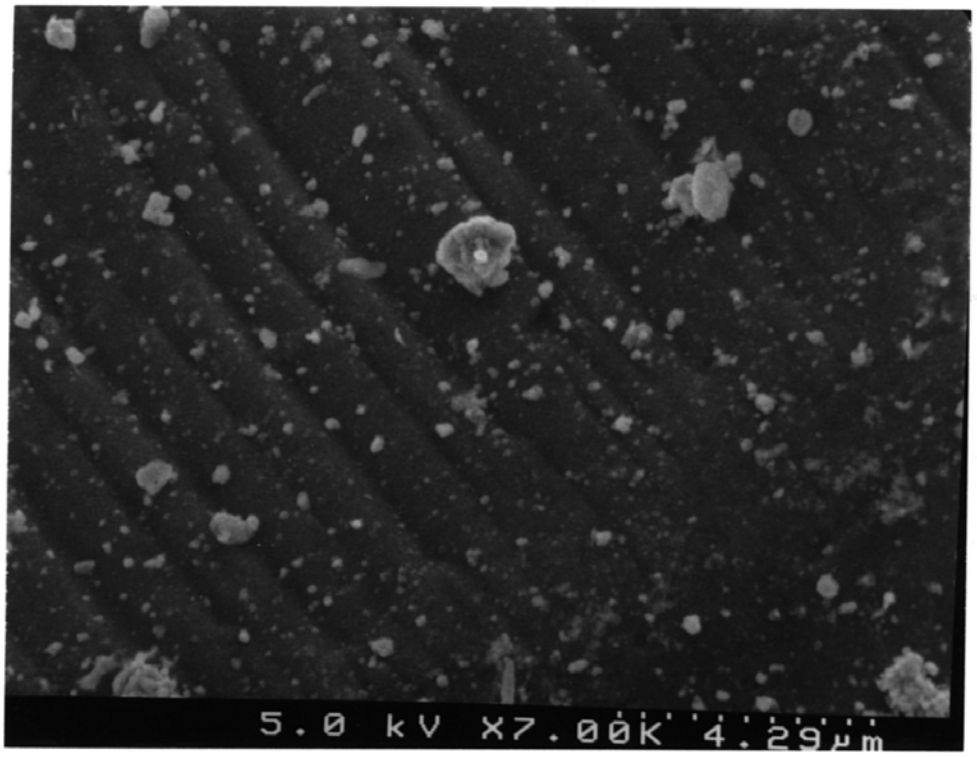

(a)

QuickTime™ and a
TIFF (LZW) decompressor
are needed to see this picture.

(b)

Figure 10

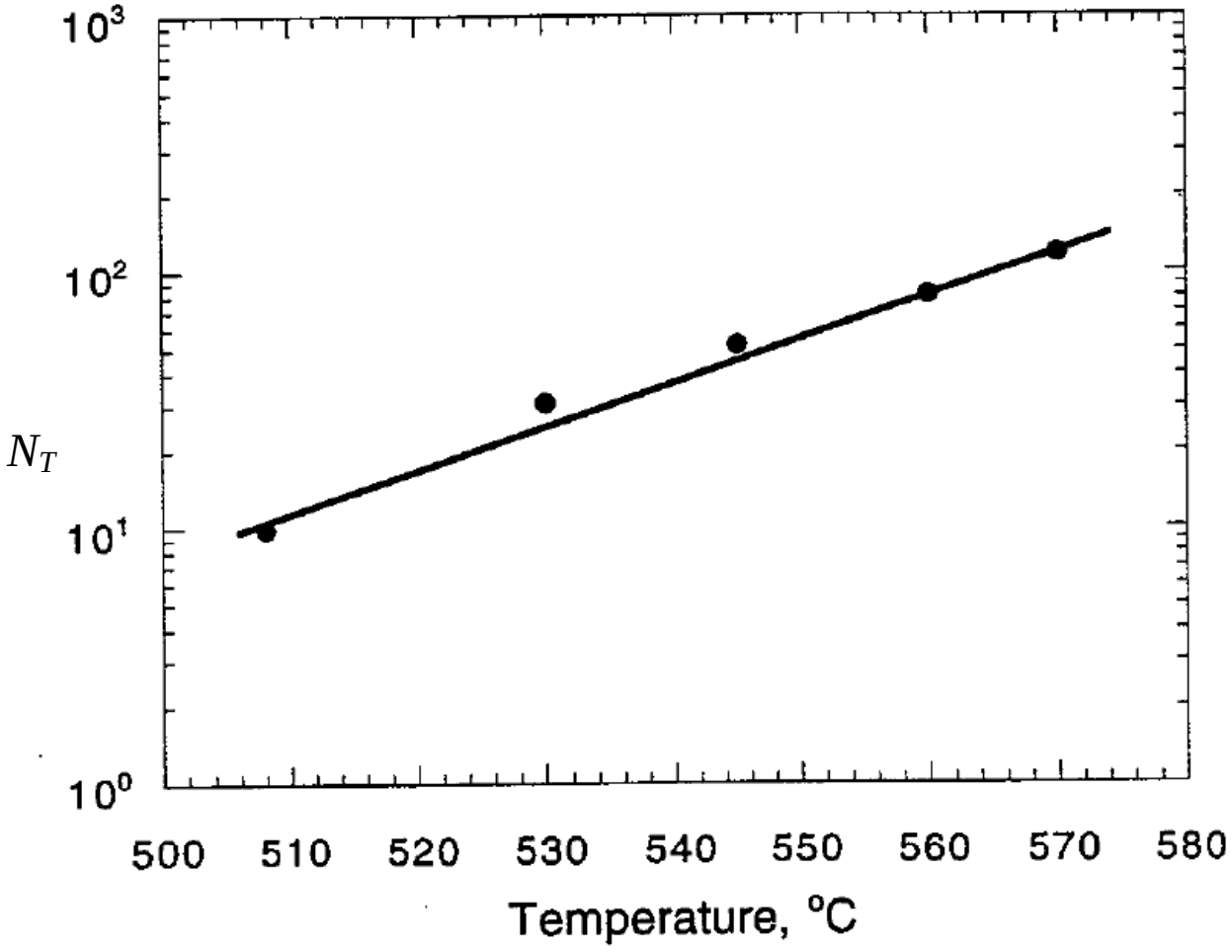
10^3
10^2
10^1
10^0
N_T
500
510
520
530
540
550
560
570
580
Temperature, °C

Figure 11

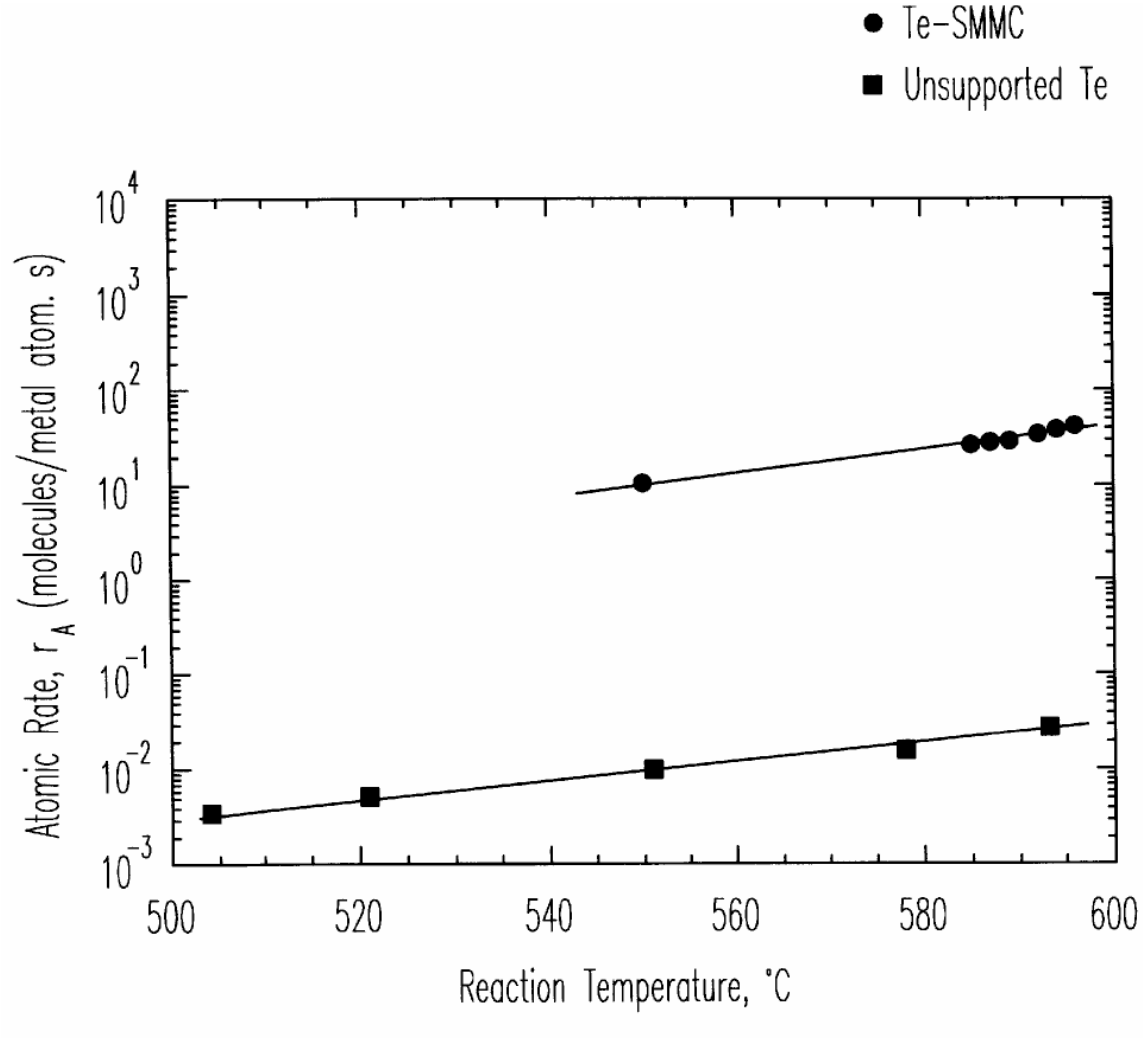
Te-SMMC
Unsupported Te
Atomic Rate, r_A (molecules/metal atom. s)
10^4
10^3
10^2
10^1
10^0
10^{-1}
10^{-2}
10^{-3}
500
520
540
560
580
600
Reaction Temperature, °C

Figure 12

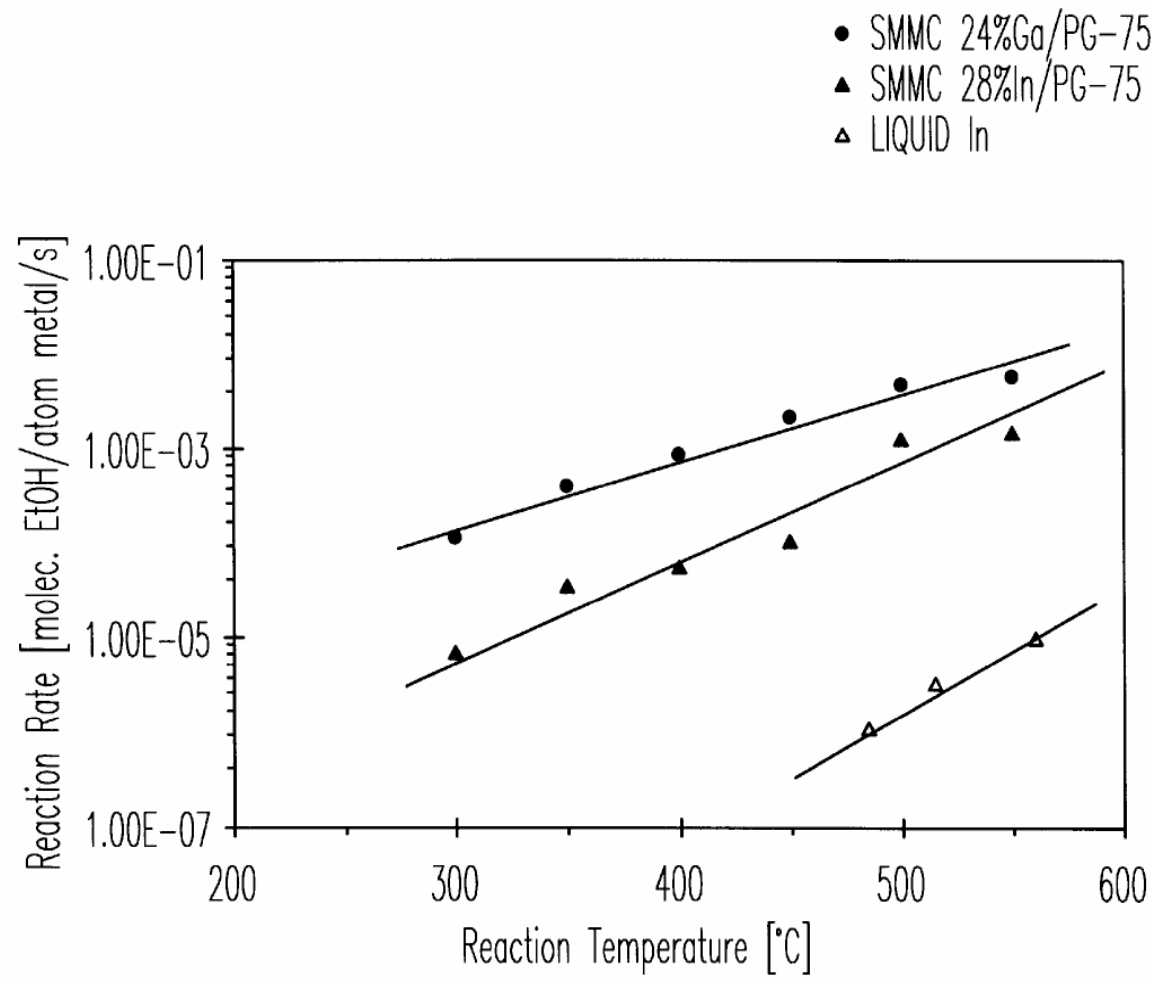
SMMC 24%Ga/PG-75
SMMC 28%In/PG-75
LIQUID In
Reaction Rate [molec. EtOH/atom metal/s]
1.00E-01
1.00E-03
1.00E-05
1.00E-07
200
300
400
500
600
Reaction Temperature [°C]

Figure 13

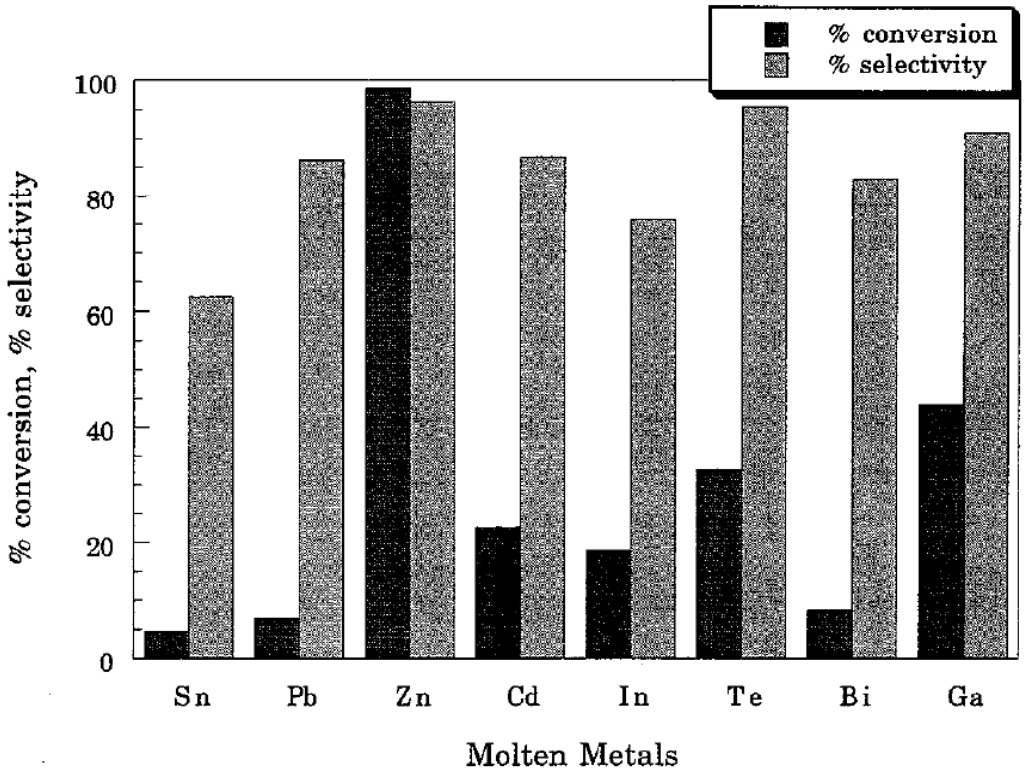
% conversion
% selectivity
100
80
60
40
20
0
% conversion, % selectivity
Sn
Pb
Zn
Cd
In
Te
Bi
Ga
Molten Metals

(a)

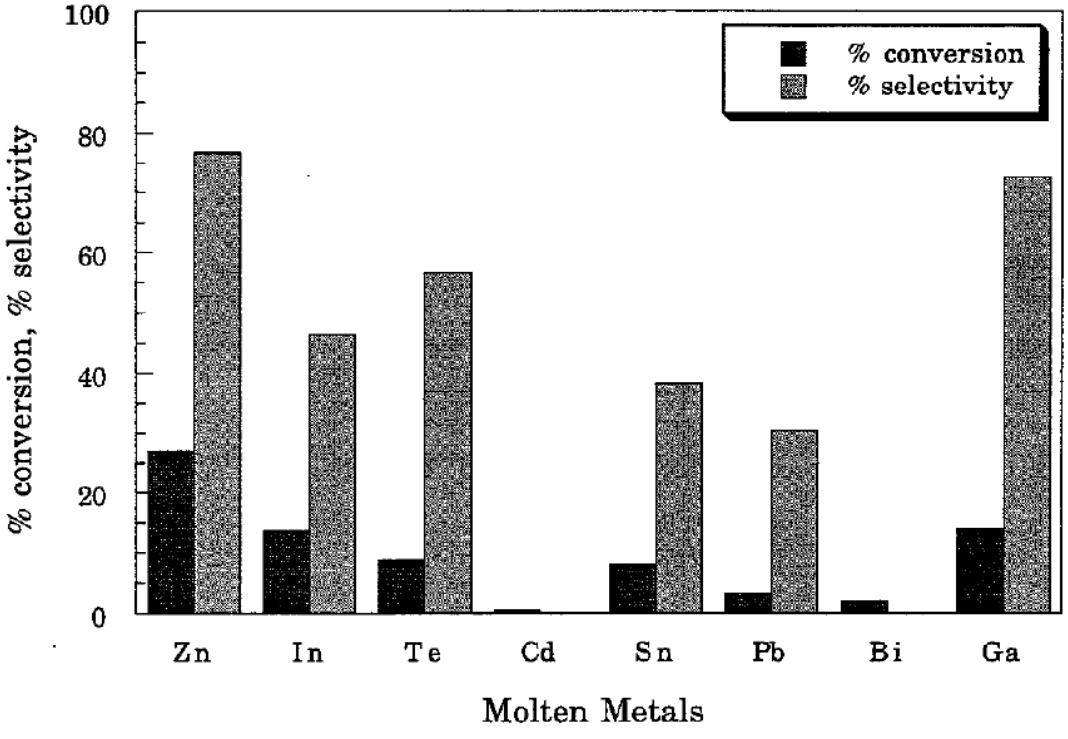
% conversion
% selectivity
100
80
60
40
20
0
% conversion, % selectivity
Zn
In
Te
Cd
Sn
Pb
Bi
Ga
Molten Metals

(b)

Figure 14

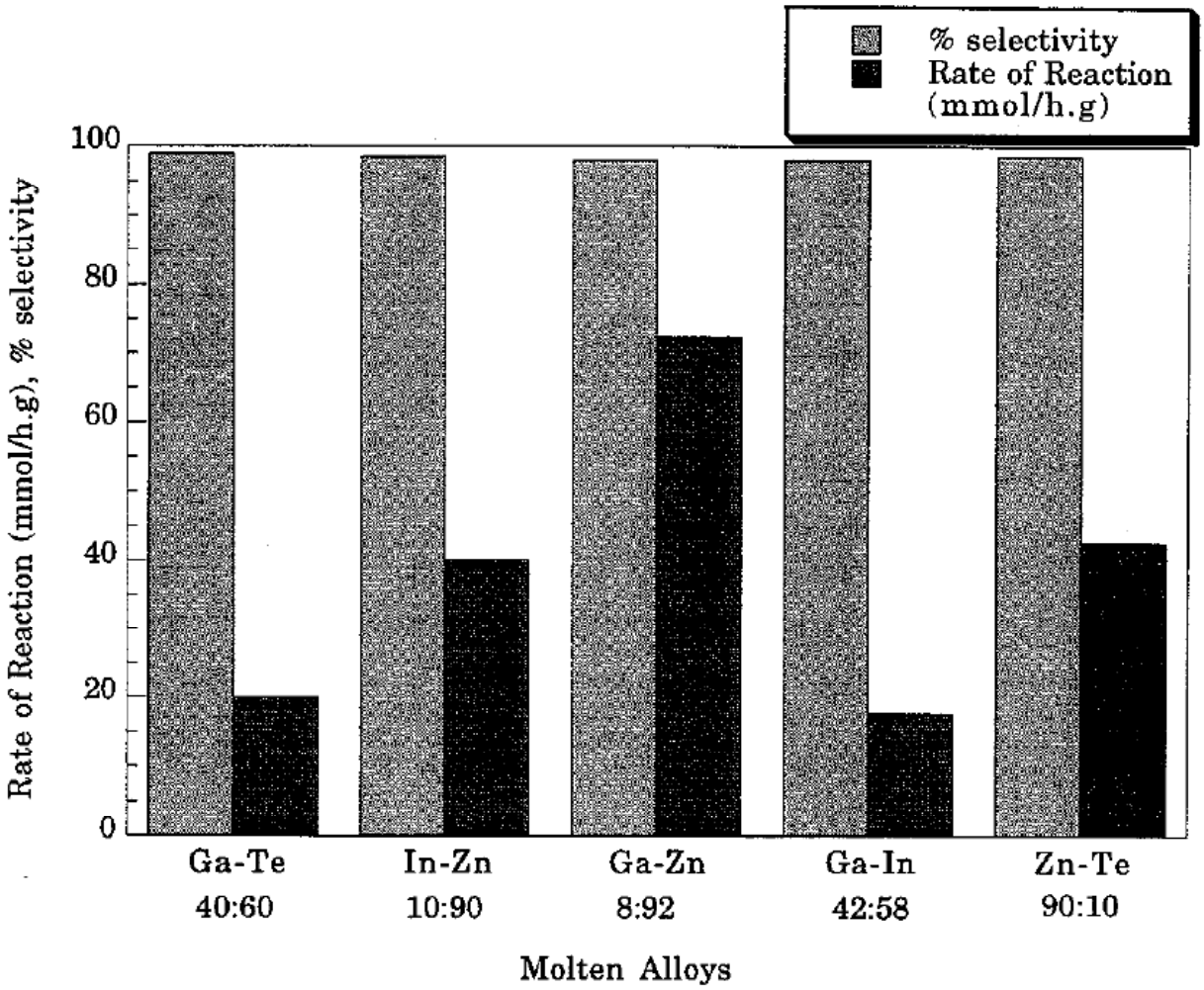
% selectivity
Rate of Reaction (mmol/h.g)
Rate of Reaction (mmol/h.g), % selectivity
100
80
60
40
20
0
Ga-Te 40:60
In-Zn 10:90
Ga-Zn 8:92
Ga-In 42:58
Zn-Te 90:10
Molten Alloys

Figure 15

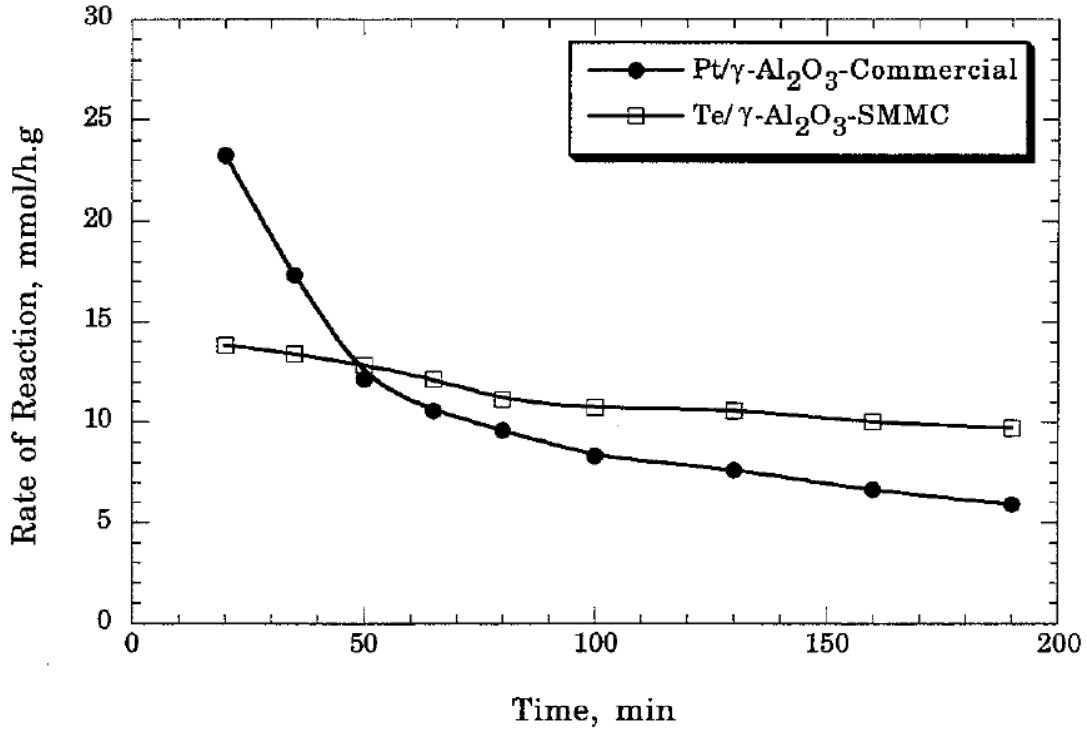
Pt/γ-Al2O3-Commercial
Te/γ-Al2O3-SMMC
Rate of Reaction, mmol/h.g
Time, min
0
5
10
15
20
25
30
0
50
100
150
200

(a)

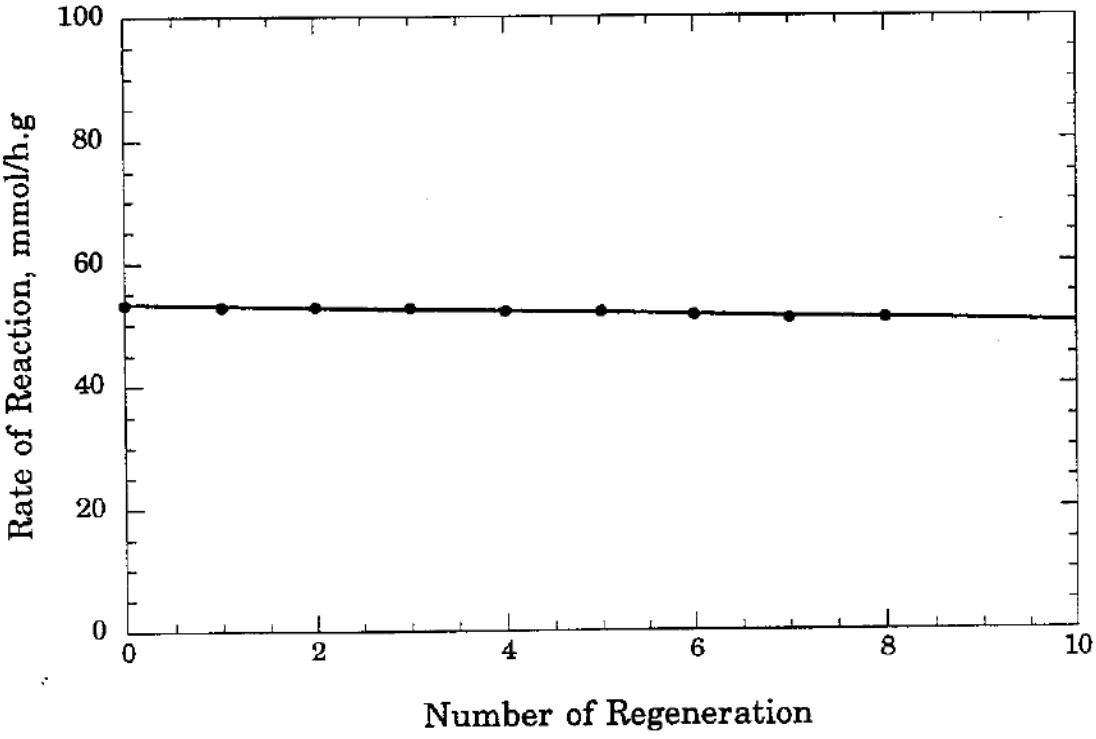
Rate of Reaction, mmol/h.g
Number of Regeneration
0
20
40
60
80
100
0
2
4
6
8
10

(b)

Figure 16

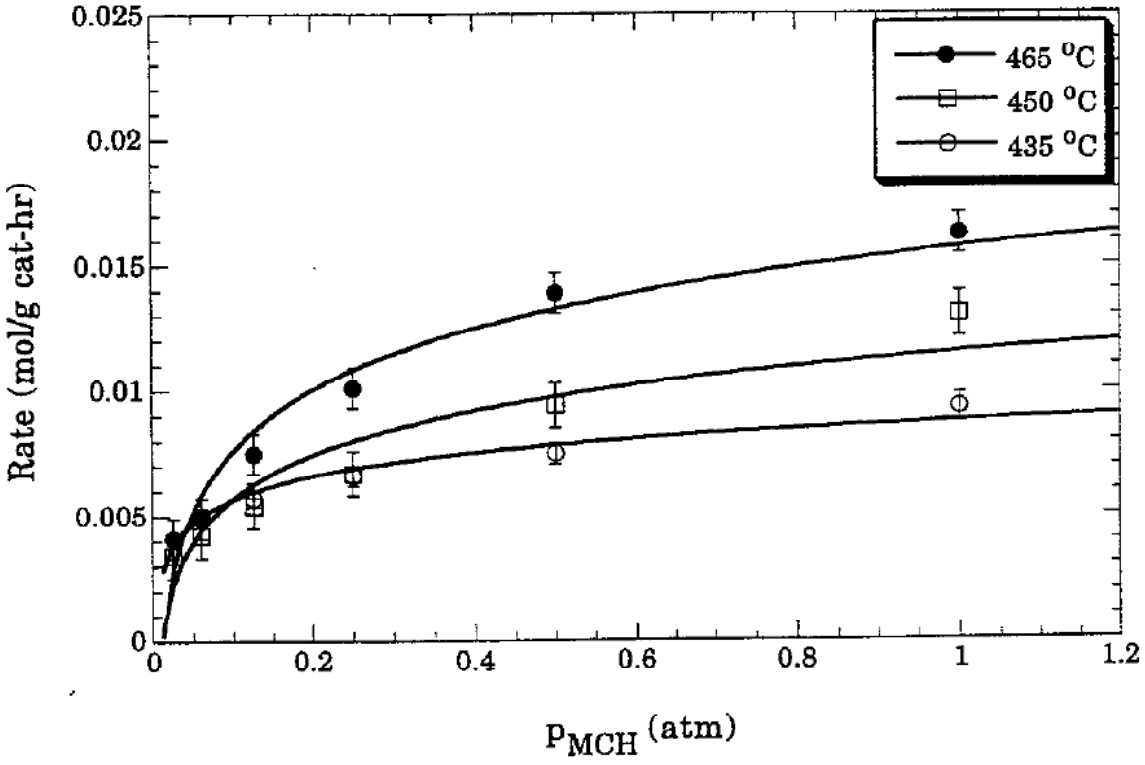
0.025
0.02
0.015
0.01
0.005
0
Rate (mol/g cat-hr)
0
0.2
0.4
0.6
0.8
1
1.2
p_{MCH} (atm)
465 °C
450 °C
435 °C

(a)

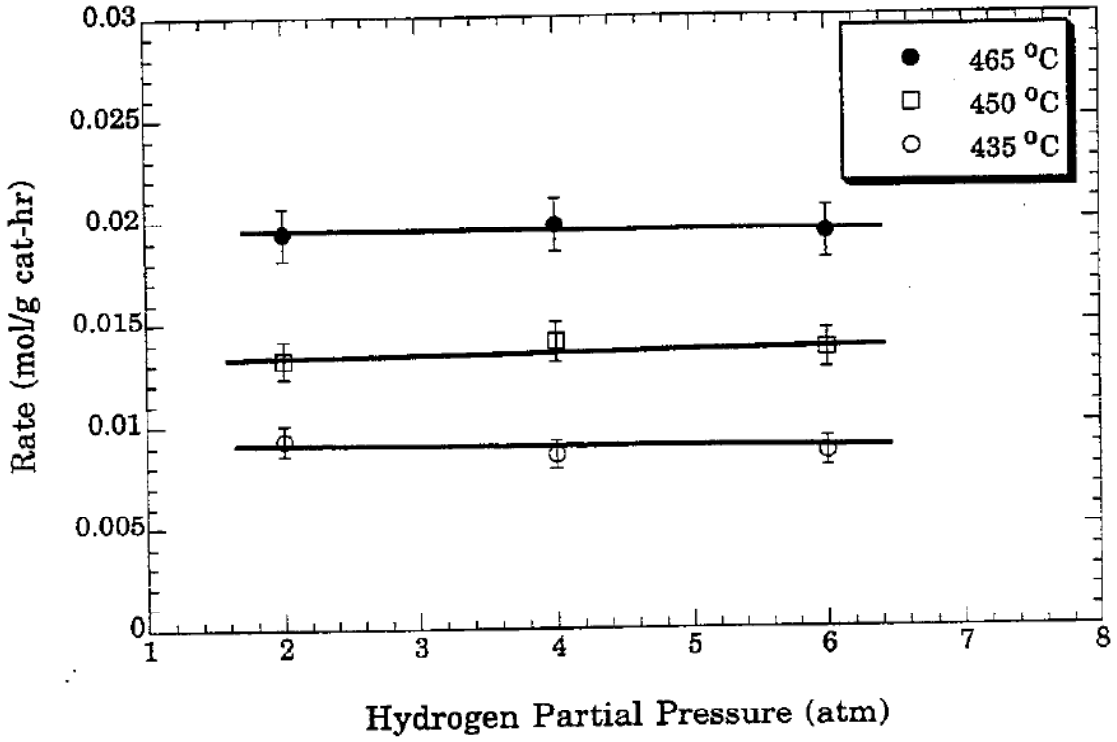
0.03
0.025
0.02
0.015
0.01
0.005
0
Rate (mol/g cat-hr)
1
2
3
4
5
6
7
8
Hydrogen Partial Pressure (atm)
465 °C
450 °C
435 °C

(b)

Figure 17

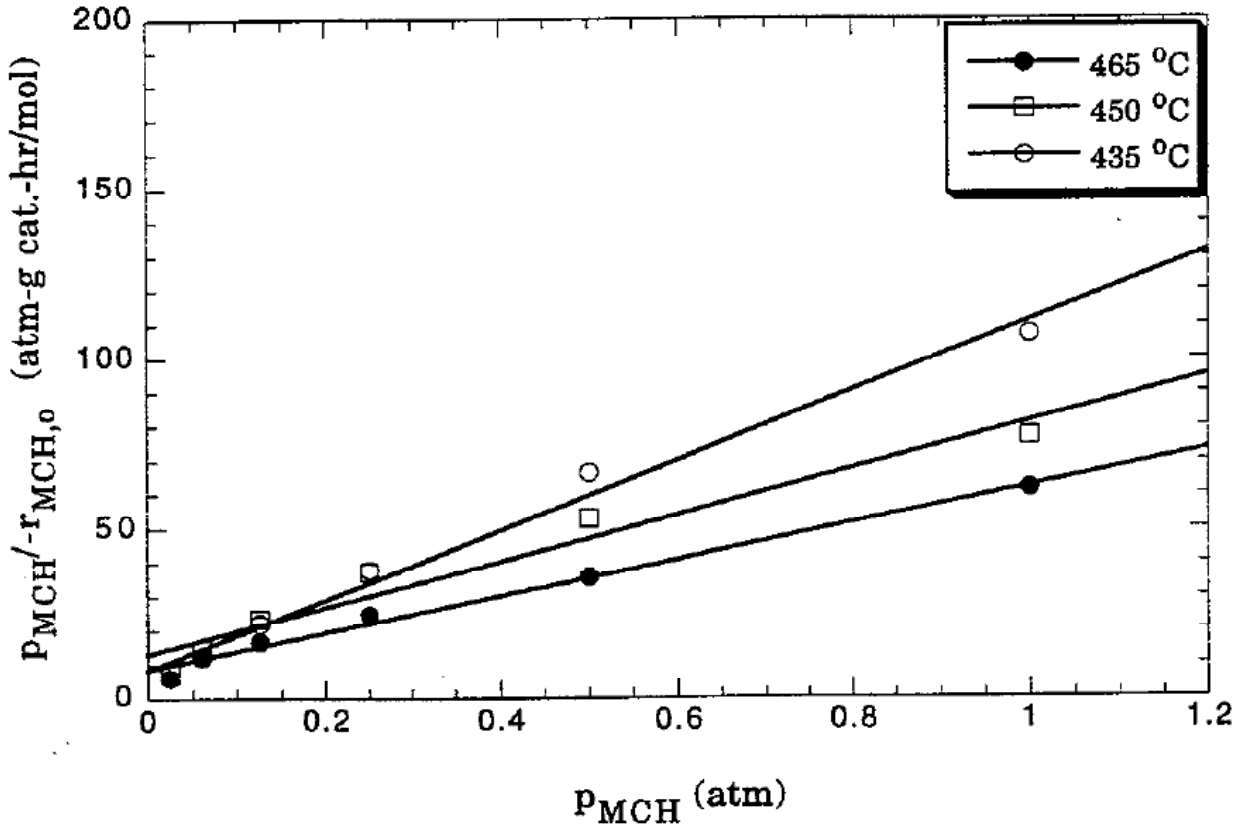
200
150
100
50
0
0
0.2
0.4
0.6
0.8
1
1.2
465 °C
450 °C
435 °C
$p_{MCH}/-r_{MCH,o}$ (atm-g cat.-hr/mol)
p_{MCH} (atm)

Figure 18

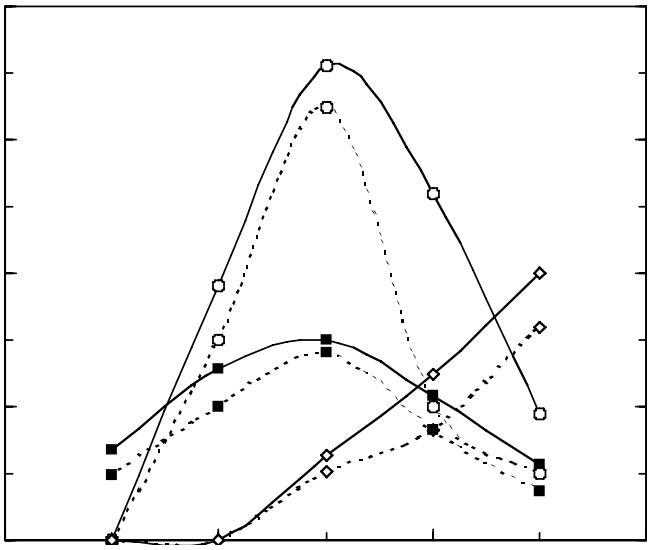

(a)

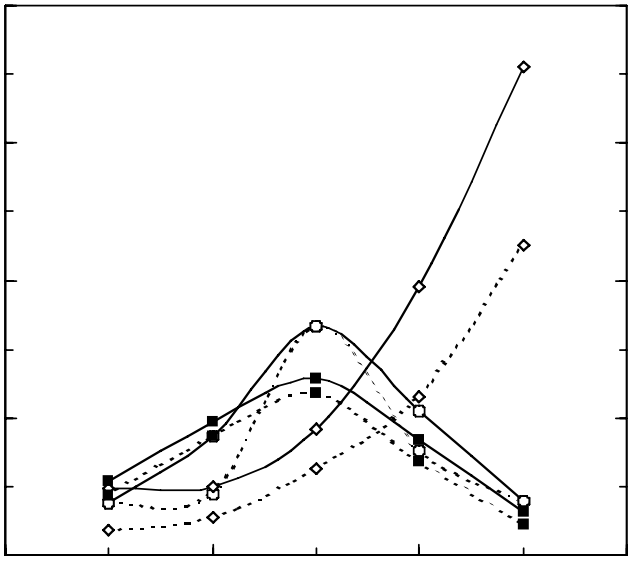

(b)

Figure 19

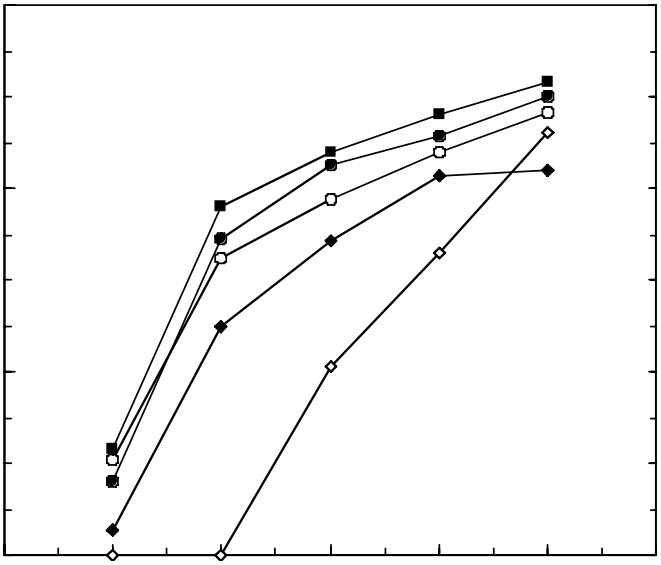

(a)

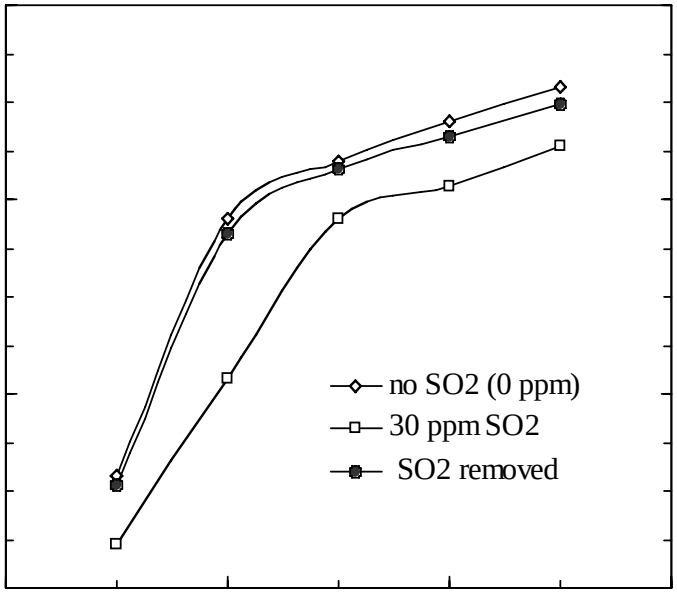

(b)

Figure 20